HHS Public Access

Author manuscript

Cell Metab. Author manuscript; available in PMC 2020 September 03.

Published in final edited form as:

Cell Metab. 2019 September 03; 30(3): 573–593.e8. doi:10.1016/j.cmet.2019.06.018.

Identification and application of gene expression signatures associated with lifespan extension

Alexander Tyshkovskiy[1,2,3], **Perinur Bozaykut**[1], **Anastasia A. Borodinova**[4], **Maxim V. Gerashchenko**[1], **Gene P. Ables**[5], **Michael Garratt**[6], **Philipp Khaitovich**[2,7,8,9], **Clary B. Clish**[10], **Richard A. Miller**[6], **Vadim N. Gladyshev**[1,10,11,*]

[1]Division of Genetics, Department of Medicine, Brigham and Women's Hospital, Harvard Medical School, Boston, MA 02115, USA

[2]Center for Data-Intensive Biomedicine and Biotechnology, Skolkovo Institute of Science and Technology, Moscow, 143028, Russia

[3]Belozersky Institute of Physico-Chemical Biology, Moscow State University, Moscow 119234, Russia

[4]Institute of Higher Nervous Activity and Neurophysiology, Russian Academy of Sciences, Moscow, 117485, Russia

[5]Orentreich Foundation for the Advancement of Science, Inc., Cold Spring, NY, USA

[6]Department of Pathology and Geriatrics Center, University of Michigan, Ann Arbor, MI 48109, USA

[7]Comparative Biology group, CAS-MPG Partner Institute for Computational Biology, 320 Yue Yang Road, Shanghai, 200031, China

[8]Max Planck Institute for Evolutionary Anthropology, Deutscher Platz 6, Leipzig, 04103, Germany

[9]School of Life Science and Technology, Shanghai Tech University, Shanghai, 200031, China

[10]Broad Institute, Cambridge, MA

[11]Lead Contact

SUMMARY

Several pharmacological, dietary and genetic interventions that increase mammalian lifespan are known, but general principles of lifespan extension remain unclear. Here, we performed RNAseq

*Correspondence should be addressed to V.N.G. (vgladyshev@rics.bwh.harvard.edu).

AUTHOR CONTRIBUTIONS

A.T. and V.N.G. designed the research; A.T. performed the research and data analysis; G.P.A. and R.A.M. performed animal experiments; A.T., P.B., M.V.G., A.A.B. and C.B.C. prepared samples for RNA sequencing and metabolite profiling; P.B., M.V.G. and P.K. contributed new reagents/analytic tools; V.N.G. supervised all aspects of the study; A.T. and V.N.G. wrote the manuscript with contributions from R.A.M., M.G., P.B., and M.V.G. All authors read the final version.

DECLARATION OF INTERESTS

The authors declare no competing interests.

analyses of mice subjected to 8 longevity interventions. We discovered a feminizing effect associated with growth hormone regulation and diminution of sex-related differences. Expanding this analysis to 17 interventions with public data, we observed that many interventions induced similar gene expression changes. We identified hepatic gene signatures associated with lifespan extension across interventions, including upregulation of oxidative phosphorylation and drug metabolism, and showed that perturbed pathways may be shared across tissues. We further applied the discovered longevity signatures to identify new lifespan-extending candidates, such as chronic hypoxia, KU-0063794 and ascorbyl-palmitate. Finally, we developed GENtervention, an app that visualizes associations between gene expression changes and longevity. Overall, this study describes general and specific transcriptomic programs of lifespan extension in mice and provides tools to discover new interventions.

Graphical Abstract

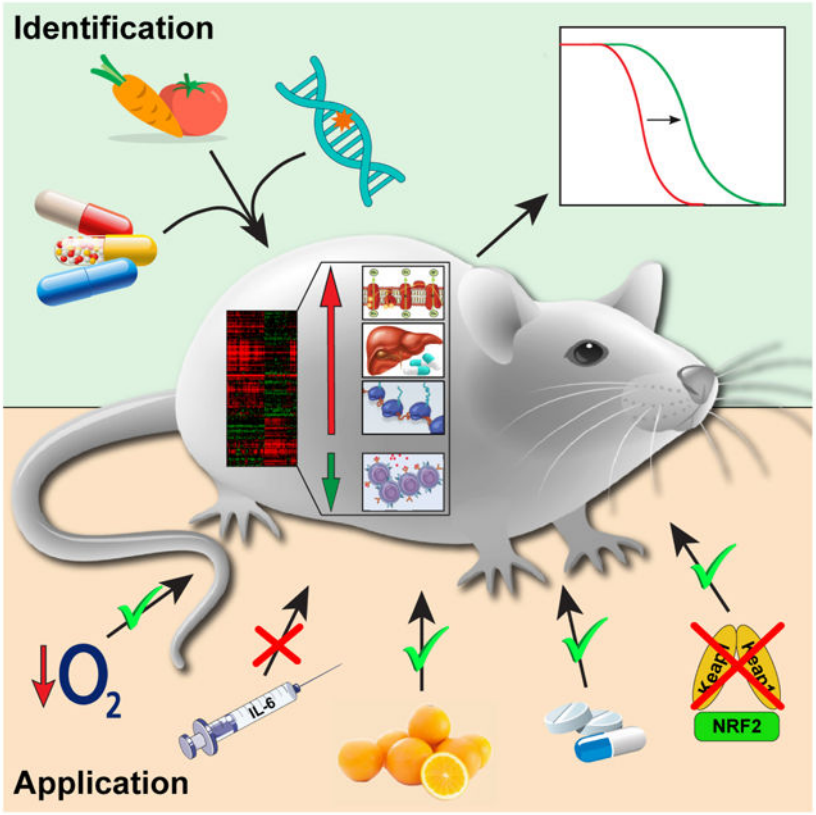

eTOC blurb (In Brief)

Tyshkovskiy et al. performed a comprehensive analysis of 17 known lifespan-extending interventions in mice at the level of gene expression to better understand general principles of lifespan control and generate gene expression signatures associated with longevity. They applied these signatures to predict new candidate compounds for lifespan extension.

Keywords

aging; longevity; lifespan extension; lifespan-extending interventions; growth hormone; rapamycin; caloric restriction; feminizing effect; longevity signatures; gene expression; GENtervention

INTRODUCTION

Dozens of pharmacological, genetic and dietary interventions that lead to lifespan extension are known today for organisms ranging from yeast to mammals (Fontana et al., 2010). They include certain mutations such as *eat-2* (Lakowski and Hekimi, 1998) and growth hormone receptor knockout (GHRKO) (Zhou et al., 1997), drugs such as rapamycin (Harrison et al., 2009) and 17-α-estradiol (Harrison et al., 2014) and diets such as caloric restriction (CR) (David et al., 1971; Houthoofd and Vanfleteren, 2006; Lin et al., 2000; Weindruch et al., 1986) and methionine restriction (MR) (Richie et al., 1994). Every year, 3-5 pharmacological interventions are tested for the longevity effects in a multi-institutional study, the interventions testing program (ITP) (Miller et al., 2007). The ITP examines the effects of compounds on mouse lifespan using large sample size and genetically heterogenous UM-HET3 animals. This experimental design makes ITP one of most reliable sources of data on longevity interventions in mice. To date, this program has shown a significant lifespan-extending effect of acarbose (Harrison et al., 2014; Strong et al., 2016), 17-α-estradiol (Harrison et al., 2014; Strong et al., 2016), Protandim™ (Strong et al., 2016), rapamycin (Harrison et al., 2009; Miller et al., 2011, 2014) and nordihydroguaiaretic acid (NDGA) (Harrison et al., 2014; Strong et al., 2016), whereas other treatments such as oxaloacetic acid, green tea extract, fish oil, resveratrol and metformin did not significantly increase lifespan at the doses used in these studies (Miller et al., 2011; Strong et al., 2013, 2016).

Interestingly, longevity interventions unequally affect different sexes. Thus, GHRKO leads to an average lifespan increase of 55% in males, but only 38% in females (Coschigano et al., 2000), whereas NDGA increases male median lifespan (by 9-12% depending on dose and age of mice), but does not affect female lifespan (Harrison et al., 2014; Strong et al., 2008). The male-only effects were also observed for 17-α-estradiol (Harrison et al., 2014; Strong et al., 2016) and Protandim (Strong et al., 2016), while *S6K1* deletion extended only female lifespan (Selman et al., 2009). Despite some differences, several key underlying molecular players and processes have been implicated, such as growth hormone (GH) receptor (Brown-borg, 2007; Coschigano et al., 2003), insulin-like growth factor 1 (IGF-1) (Brown-borg, 2007; Lopez-Otin et al., 2013), mammalian target of rapamycin (mTOR) (Kapahi et al., 2004; Vellai et al., 2003) and sirtuins (Lin et al., 2000; Lopez-Otin et al., 2013; Tissenbaum and Guarente, 2001). On the other hand, manipulation of these hubs does not necessarily lead to longevity. Thus, resveratrol, a sirtuin activator (Gertz et al., 2012), increases lifespan only in mice subjected to a high calorie diet by reducing liver pathology and providing other health benefits such as improved insulin sensitivity and motor function (Baur et al., 2006; Pearson et al., 2008). However, on a regular diet, resveratrol has no effect on lifespan despite improvement in cardiovascular function, bone density, and motor coordination (Miller et al.,

2011; Pearson et al., 2008; Strong et al., 2013). On the other hand, several lifespan-extending interventions, such as *Myc* haploinsufficiency (*Myc* +/−) (Hofmann et al., 2015), seem to bypass known hub regulators of longevity. Therefore, it remains unclear, which effects of the drug, diet, or mutant are necessary and/or sufficient for lifespan extension.

High-throughput analyses that employ transcriptomics, metabolomics or epigenomics, have been widely used to evaluate systemic effects that define the aging process. For example, they were used to examine unique features of long-lived species, such as naked mole rats (Zhao et al., 2018), association with lifespan across mammals (Fushan et al., 2015; Ma et al., 2015, 2016) and changes occurring in organisms during the aging process (Sziráki et al., 2018). Certain healthspan- and lifespan-extending interventions have also been analyzed at systemic level. For example, metformin (Martin-Montalvo et al., 2013), rapamycin (Fok et al., 2014a), CR (Rusli et al., 2015), GHRKO (Rowland et al., 2005), Snell dwarf, Ames dwarf (Boylston et al., 2006), *S6K1* deletion (Selman et al., 2009), *Myc* +/− (Hofmann et al., 2015) and *Fgf21* overexpression (Zhang et al., 2012) have all been investigated at the level of gene expression. This revealed differentially expressed genes and molecular pathways perturbed in response to a particular intervention. Some of these interventions, such as rapamycin and CR (Fok et al., 2014b), Little and Ames dwarf mice (Amador-Noguez et al., 2004), and CR and Ames dwarf mice (Tsuchiya et al., 2004), have also been analyzed together at proteomic and transcriptomic levels. These studies revealed individual genes and molecular pathways shared by certain pairs of interventions. For example, CR and Ames dwarf mice were both shown to upregulate the expression of genes encoding xenobiotic-metabolizing and lipid beta-oxidation enzymes (Tsuchiya et al., 2004). However, focusing on narrow subsets of interventions did not allow to arrive at general patterns of lifespan-extending conditions.

Extensive transcriptome data corresponding to different longevity interventions are available in public databases. Using this resource, several studies conducted meta-analyses of CR at the level of gene expression (Plank et al., 2012; Swindell, 2008), identifying persistent and reliable patterns altered across different experimental settings in response to a single longevity intervention. Nonetheless, thorough analyses examining a wide range of lifespan-extending interventions have essentially been lacking. Here, we fill this gap by performing systemic gene expression analysis of mouse liver subjected to more than a dozen of longevity interventions across different experimental settings. First, we obtained RNAseq data for 8 different lifespan-extending interventions, including well-studied ones, such as CR, rapamycin and GHRKO, as well as those that have never been analyzed at the transcriptomic level, across different sexes, doses and age groups. We then aggregated our dataset with publicly available data, which resulted in the coverage of 17 interventions by 77 datasets across 22 different sources, and performed an analysis of gene expression changes associated with lifespan extension.

RESULTS AND DISCUSSION

RNAseq of hepatic responses to longevity intervention

We subjected 78 young adult mice to 8 interventions previously established to extend lifespan, including acarbose, 17-α-estradiol, rapamycin, Protandim, CR (40%), MR (0.12%

methionine w/w), GHRKO and *Pit1* knockout (Snell dwarf mice) (Fig. 1A, Table S1A). This set included three interventions that have never been analyzed at the level of gene expression (acarbose, 17-α-estradiol and Protandim). All compounds and diets were applied to genetically heterogeneous UM-HET3 mice and started at 4 months of age, as in ITP studies (Harrison et al., 2014; Miller et al., 2011, 2014; Strong et al., 2016), except for MR, which was applied to 2-month-old C57BL6/J mice, as in (Ables et al., 2012, 2015). We then performed RNAseq on liver samples of these mice, together with sex- and age-matched littermate controls, analyzing both males and females in most cases. Since some of these interventions are known to be effective when used at different concentrations and different ages (Harrison et al., 2009, 2014; Mercken et al., 2014a; Miller et al., 2014; Mitchell et al., 2016; Strong et al., 2016), we also used 2 different age groups for CR, rapamycin and acarbose, and 2 different effective concentrations of rapamycin (Fig. 1A). As age- and lifespan-associated patterns may or may not correlate with each other, and we aimed to identify signatures of lifespan extension apart from the changes related to the consequences of slowed down aging, all mice utilized in these experiments were young and middle-aged. This allowed us to attribute the observed gene expression changes to the direct effect of lifespan-extending interventions and to analyze longevity patterns independent of the aging process.

Differentially expressed genes associated with each intervention were initially examined separately for males and females. Many of them were found to be shared by different interventions. Thus, almost half of MR genes (44.3% up- and 41.8% downregulated genes) were altered significantly and in the same direction in Snell dwarf males and mice subjected to CR (Fig. 1B). This observation is consistent with findings that the lifespan extension effect of CR in flies is dependent on methionine in the diet and can be abrogated by the addition of amino acids including methionine (Grandison et al., 2009).

Functional enrichment analysis also revealed many similarities among the interventions (Fig. 1D, Table S2). For example, many ribosomal protein genes were upregulated in response to all interventions except MR (q-value < 0.001). Other commonly upregulated functions included drug metabolism by cytochrome P450, glutathione metabolism, oxidative phosphorylation and TCA cycle. In addition to common mechanisms, we also detected some distinct patterns. For example, 17-α-estradiol in females and MR induced downregulation of oxidative phosphorylation, and fatty acid oxidation, which was known to be positively associated with the lifespan extension effect of several interventions in males (Amador-Noguez et al., 2004; Plank et al., 2012; Tsuchiya et al., 2004), was significantly downregulated in females subjected to 17-α-estradiol, acarbose and CR (Fig. 1D). At the same time, this pattern was not observed in males and even demonstrated an opposite effect in case of acarbose and CR.

Interestingly, although MR mice shared many differentially expressed genes with CR and interventions associated with GH deficiency (i.e., GHRKO and Snell dwarf mice), they displayed a distinct pattern at the level of functional enrichment compared to other interventions (Fig. 1C, S1A). MR shared some common signatures with CR and GH-deficient mutants, including upregulation of glutathione metabolism and drug metabolism by

cytochrome P450, but also exhibited upregulation of mTOR pathway and downregulation of oxidative phosphorylation, which was distinct from most other interventions (Fig. 1D).

Feminizing effect of lifespan-extending interventions

The finding of sex-specific gene expression patterns for certain interventions allowed us to examine this question in more detail. Several previous studies noted a feminizing effect of CR and GH deficiency on gene expression in males (Buckley and Klaassen, 2009; Estep et al., 2009; Fu and Klaassen, 2014; Li et al., 2013). To test if this effect is reproduced across different interventions, we first identified genes whose expression significantly differed between control males and females in both 6- and 12-month-old age groups (Table S3A). We then examined how lifespan-extending interventions affect these sex-associated differences.

In males, we detected statistically significant feminizing patterns for genetic (GHRKO and Snell dwarf mice) and dietary (CR and MR) interventions at the level of gene expression (Fig. 2B, Table S3C). In other words, each of these interventions upregulated female-specific and downregulated male-specific genes. For example, female- and male-associated expression patterns shared more than 66% of up- and 72% of downregulated genes, respectively, that were perturbed by GHRKO and 6-month-old CR in males and showed a statistically significant overlap with both (Fisher exact test adjust p-value < $2.98 \cdot 10^{-18}$) (Fig. 2A). The feminizing effect was especially strong for genetic mutants, reaching 80% correlation for GHRKO (Spearman correlation test adjusted p-value = $6.1 \cdot 10^{-56}$; Fig. S1B). Besides mutants and diets, acarbose and rapamycin also produced the feminizing effect in males for one of age groups (adjusted p-value < $4.1 \cdot 10^{-3}$). However, other drugs did not induce a significant feminizing effect in males or even resulted in a slight negative effect, e.g. Protandim in 6-month-old mice (Spearman correlation = −0.11; BH adjusted p-value = 0.088; Fig. 2B).

In females, the effect of interventions on sex-specific genes was mostly similar to that in males. Thus, CR and 12-month-old acarbose also exhibited a significant feminizing pattern (adjusted p-value < 0.07). (Fig. 2B). On the other hand, rapamycin produced a significant anti-feminizing (“masculinizing”) pattern in females in both age groups (Spearman correlation < −0.14, adjusted p-value < 0.04), upregulating male-specific and downregulating female-specific genes. Interestingly, one of the strongest masculinizing patterns in females was produced by 17-α-estradiol, which had no significant effect on sex-associated genes in males, hinting that its selective effect on male lifespan is not due to simple recapitulation of the female hormonal profile. Our data suggest that feminization does not explain the effect of interventions on lifespan extension. Indeed, 17-α-estradiol didn’t lead to feminizing changes in males but increased their median (by 19%) and maximum (by 12%) lifespan (Strong et al., 2016). At the same time, Protandim produced a significant feminizing effect in females, but didn’t extend lifespan in ITP studies (Strong et al., 2016). Besides, in females rapamycin and 17-α-estradiol showed a similar and significant masculinizing effect, although only the former extended lifespan in females, and its effect was even greater than that in males (Miller et al., 2014). Therefore, it seems that feminization (or masculinization) are neither necessary nor sufficient for lifespan extension,

although many interventions, including GH mutants and diets, influence some of the genes associated with gender-specific differences.

Although various interventions had a different effect on sex-specific genes, we observed a consistently stronger feminizing effect in males compared to females for every individual intervention and age group (Spearman correlation test adjusted p-value < $2.6 \cdot 10^{-6}$), except for Protandim (Fig. 2B). In other words, regardless of the direction and size of the effect of particular interventions on sex-associated genes in males, most of them led to relatively more masculinizing changes in females. To test if such pattern results in the convergence of gender-associated gene expression profiles to some neutral state, we calculated pairwise distances between expression of these genes in male and female samples for all experimental groups (Fig. 2C). We found that sex-associated differences were indeed significantly reduced by all interventions, except for 6-month Protandim and 12-month rapamycin (Mann-Whitney test adjusted p-value < 0.024). This finding suggests that the state induced by lifespan-extending interventions is broadly shared across sexes, with differences between males and females becoming less prominent.

To better understand the nature of the feminizing pattern, we identified sex-associated genes, which change in response to interventions is, at the same time, associated with the feminizing effect. With the FDR threshold of 0.05 and FC threshold of 1.5, we detected 355 sex-associated genes differentially expressed at a higher level in females and 282 genes expressed at a lower level (Fig. 2F). Among them, 153 (out of 355) and 164 (out of 282) genes were positively and negatively associated with the feminizing effect, respectively. Functional enrichment of these genes revealed upregulation of drug metabolism (Fisher exact test adjusted p-value = $1.5 \cdot 10^{-9}$) and fatty acid metabolism (Fisher exact test adjusted p-value = 0.026) (Fig. 2G). Cytochrome P450 genes, involved in drug metabolism, are well known to be differentially expressed between sexes in mice and regulated by GH and its sex-specific daily pulse frequency and amplitude (Waxman and Holloway, 2009). However, it was previously unclear whether the same xenobiotic metabolizing enzyme (XME) genes are altered in response to different lifespan-extending interventions. Here, we show that this is indeed the case. Interestingly, male rodents also demonstrate a female-like alteration of some other sex-specific cytochrome P450s with age, both at the level of gene expression and enzymatic activity (Imaoka et al., 1991; Kamataki et al., 1985). This appears to be, at least partly, due to the change of their GH secretion profile (Imaoka et al., 1991; Wauthier et al., 2007). Therefore, feminization of the drug metabolism system in males seems to be an example of the pattern positively associated with both aging and response to several lifespan-extending interventions.

Among downregulated sex-associated genes, we detected enrichment of complement and coagulation cascades (Fisher exact test adjusted p-value = $9.8 \cdot 10^{-3}$) and major urinary proteins (MUP) genes (Fisher exact test adjusted p-value = 0.021) (Fig. 2G). MUP expression is highly sex-specific, and the high concentration of total and specific MUP proteins in male mouse urine appears to influence male attractiveness to females (Garratt et al., 2011; Roberts et al., 2010), suggesting a possible link between lifespan extension and reproductive fitness. Interestingly, sexually dimorphic expression of most MUP isoforms is also known to be regulated by GH. Indeed, *Mup* genes are significantly downregulated in

GH-deficient mutants, but their level can be restored by GH injection (Knopf et al., 1983). Moreover, injection of GH could masculinizes MUP mRNA levels in female mice (al-Shawi et al., 1992). Therefore, gene expression changes associated with the feminizing effect across interventions are generally linked to GH as a key upstream regulator.

To validate our findings, we performed metabolite profiling of 39 12-month-old male and female mice subjected to control diet, acarbose or rapamycin (Data S1, Table S1B). We further aggregated this data with our previous dataset, which included animals of the same age subjected to control diet, CR, acarbose and rapamycin along with male GHRKO and Snell dwarf mice (Ma et al., 2015). Using a similar procedure, we identified metabolites that significantly differ between control males and females in each of the datasets and then used them to calculate the feminizing effect at the metabolome level (Table S3B). In agreement with the gene expression data, a significant feminizing effect of genetic interventions (GHRKO and Snell dwarf mice), CR, and acarbose was observed in males (Fig. 2D, Table S3C), whereas rapamycin produced a significant feminizing effect only in one of the datasets. Applied to females, the same interventions also resulted in a significantly more masculinizing effect compared to males, except for rapamycin from the previously obtained dataset (adjusted p-value < 0.098). Finally, in agreement with the gene expression findings, all interventions, except for rapamycin from the new dataset, showed a reduction of sex-related differences at the metabolome levels following introduction of lifespan-extending interventions (Mann-Whitney test adjusted p-value < 0.011) (Fig. 2E).

Signatures of CR, rapamycin and growth hormone deficiency

To obtain a comprehensive picture of gene expression responses to interventions, we collected all publicly available microarray datasets for mouse liver and conducted a meta-analysis across aggregated data (Table S1C). We first focused on 3 interventions: CR, rapamycin and interventions related to GH deficiency (GHRKO, Little mice, Snell and Ames dwarf mice). The latter group was combined, because these interventions, although targeting different genes involved in GH production and sensing, resulted in a similar effect on the liver being unable to activate GHR. In addition, similarity among these interventions could be seen at the level of hepatic gene expression (Amador-Noguez et al., 2004) (Fig. 3F, 4C). As these intervention groups appeared to be best-studied, we were interested in the identification of consistent gene expression signatures associated with them. For this reason, we combined all data across sexes, strains, ages, durations of interventions and doses. In total, we aggregated data from 29 CR datasets (across 13 studies), 9 rapamycin datasets (across 3 studies) and 20 GH deficiency datasets (across 7 studies) (Table S1).

To overcome issues associated with differences in platforms across studies and batch effects, we developed an integrative method based on independent preprocessing of individual datasets and subsequent aggregation of mean logFC and their standard deviations for all genes detected in our RNAseq data. Importantly, to account for possible differences in the general effect of interventions on mouse transcriptome, we did not normalize distributions of logFC across datasets. To include information about standard deviations of logFC and account for possible batch effects due to the use of several datasets sharing the same control, we applied a mixed-effect model. We used this approach to identify genes up- or

downregulated across datasets associated with the same type of intervention. Instead of the comparison of lists of differentially expressed genes (Plank et al., 2012; Swindell, 2008), our method accounts for the degree of the effect and variance of gene expression changes within each dataset. Besides standard p-value obtained from the mixed-effect model test, we also calculated “leave-one-out” (LOO) p-value, being the highest p-value after removal of every study one by one.

In this procedure, genes were designated statistically significant if their adjusted p-value was < 0.01 and LOO p-value was < 0.01. With these thresholds, we identified 419 up- and 370 downregulated genes for CR, 894 up- and 879 downregulated genes for GH deficiency, and 127 up- and 100 downregulated genes for rapamycin (Fig. 3A). Interestingly, CR and GH-deficient interventions significantly overlapped (37% of up- and 26.3% of downregulated genes in response to CR were shared with GH mutants; Fisher exact test p-value < 10^{-28} for both up- and downregulated genes), whereas rapamycin did not show a statistically significant overlap with either of them. Upregulated genes shared by CR and GH deficiency were enriched for oxidative phosphorylation (Fisher exact test adjusted p-value = $1.52 \cdot 10^{-9}$), and downregulated genes were enriched for complement and coagulation cascades (Fisher exact test adjusted p-value = $5.21 \cdot 10^{-6}$). The difference in the gene expression response between CR and rapamycin was previously noted (Fok et al., 2014b; Miller et al., 2014), but was not well understood. Our data provide a case for largely distinct mechanisms by which these interventions act in the liver.

Not surprisingly, all GH-deficient mutants showed downregulation of *Igf1* (Fig. S2A) and its stabilizer *Igfals* along with upregulation of 2 genes encoding its inhibitors, IGF-binding proteins *Igfbp1* and *Igfbp2* (Fig. S2B). Interestingly, *Igf1* expression showed no consistent significant changes in response to CR and rapamycin (Fig. S2A). Moreover, we did not detect a dependence of *Igf1* fold change in response to CR with any other feature, including age of mice, duration of treatment, restriction level and even the effect on lifespan. On the other hand, IGF1 plasma levels are known to be decreased by CR in various mouse models (Mitchell et al., 2016). However, the same models integrated in our meta-analysis didn’t show consistent downregulation of hepatic *Igf1*. On the other hand, we detected upregulation of two IGF1 binding partners (*Igfbp1* and *Igfbp2*) in response to CR (Fig. S2B). Therefore, inhibition of the IGF1 pathway by CR doesn’t appear to be mediated by the direct regulation of hepatic *Igf1* expression but may be associated with elevated levels of its inhibitors.

By applying gene set enrichment analysis (GSEA), we further identified molecular pathways shared by 2 or all 3 analyzed interventions (Fig. 3B; Table S4A). Interestingly, rapamycin was found to share some perturbed functions with other interventions, in agreement with the RNAseq data. Thus, oxidative phosphorylation was commonly upregulated across all three interventions (q-value < 0.008). Other shared upregulated functions included TCA cycle, ribosome and genes associated with age-related diseases (Parkinson’s and Huntington’s).

To identify upstream regulators of observed gene expression changes, we performed enrichment analysis of transcription factors using TRANSFAC (Matys, 2006). First, for each individual dataset we identified transcription factor binding to sequences enriched in promoters of genes differentially expressed in the corresponding dataset. We then applied a

binomial test to identify factors whose enrichment was overrepresented across datasets within the same type of intervention. A permutation FDR threshold of 0.01 allowed us to identify 161 transcription factor IDs enriched for CR, 213 IDs enriched for GH-deficient interventions and 17 IDs enriched for rapamycin (Fig. 3C, Table S5). Consistent with previous results, CR and GH mutants shared more than 50% of enriched transcription factors (Fisher exact test p-value < 10^{-26}). However, here rapamycin also showed significant overlap with the other interventions (58.8% and 47.1% of transcriptional factors were shared with CR and GH deficiency, respectively; Fisher exact test p-value < 0.002 in both cases). Interestingly, 8 factors found to be enriched by all 3 interventions included receptors related to glucose sensitivity and sterol metabolism, such as glucocorticoid receptor NR3C1 and sterol regulatory element binding transcription factor SREBP-1. Factors shared by CR and GH deficiency included NRF2, PPARα, PPARγ along with a number of interferon regulatory factors, in accordance with the results of functional enrichment (Fig. 3C). Therefore, it appears that even though rapamycin exhibits a distinct pattern at the level of individual genes, its effect partly converges with other interventions at the level of molecular pathways and transcriptional regulation. A non-significant overlap of the perturbed genes observed for rapamycin may be also explained by high variability of gene expression response to this drug across different experimental settings (Fig. 4C) that is later reduced at the level of functional and transcriptional enrichment.

Mutual organization of lifespan-extending interventions

We next expanded our data by aggregating public microarray data on longevity interventions. We also included resveratrol and metformin that did not increase lifespan in the ITP mouse cohort at the concentrations used (Miller et al., 2011; Strong et al., 2013, 2016), but were found to share some molecular mechanisms with lifespan-extending CR (Barger et al., 2008; Dhahbi et al., 2005; Martin-Montalvo et al., 2013; Pearson et al., 2008), increase healthspan of mammals (Baur and Sinclair, 2006; Martin-Montalvo et al., 2013; Pearson et al., 2008) and increase lifespan of the nematode *Caenorhabditis elegans* (De Haes et al., 2014; Viswanathan et al., 2005; Wood et al., 2004), short-lived fish *Nothobranchius furzeri* (in case of resveratrol) (Valenzano et al., 2006), and mice under certain conditions (Baur et al., 2006; Martin-Montalvo et al., 2013; Pearson et al., 2008). After integration of available data, our dataset included 17 interventions and 77 control-intervention comparisons across 22 different sources (Fig. 3D). Importantly, our list of analyzed interventions covered different types of interventions, i.e. dietary, genetic (mutations, overexpression) and pharmacological (Table S1).

Data aggregation was performed using the approach discussed above. Interestingly, comparison of standard deviations of gene fold changes showed that genetic manipulations had the largest effects on gene expression (Mann-Whitney test p-value = 0.003 between dietary and genetic groups), whereas pharmacological interventions had the smallest effect (Mann-Whitney test p-value = $1.71 \cdot 10^{-6}$ between pharmacological and dietary groups), and diets were in the middle (Fig. S3A). To confirm that this effect wasn't due to technical bias, we examined possible differences between medians of gene fold changes and did not observe significant differences between any pair of intervention groups (Fig. S3B). The observed difference in the degree of the effect emphasized the importance of avoiding

normalization of mean fold changes across different datasets during data aggregation, since in that case this scale difference would be lost.

To explore how gene signatures identified for CR, GH deficiency and rapamycin are affected by other interventions, we calculated aggregated gene expression responses to each of them (Fig. 3E). In general, interventions exhibited similar transcriptomic profiles. Indeed, we observed positive Spearman correlation between aggregated gene expression changes for most interventions (Fig. 3F). Not surprisingly, GH-deficient mutants formed a tight cluster, indicating convergence of their hepatic molecular mechanisms. To examine if different interventions recapitulate the gene expression responses induced by CR, rapamycin and GH deficiency, we performed GSEA, using gene signatures of the specified interventions as input subsets (Fig. 4A). Interestingly, most interventions, including all GH-deficient mutants, diets (CR, every-other-day feeding (EOD) and MR), acarbose, FGF21 overexpression, 17-α-estradiol and resveratrol, shared the changes induced by CR and GH deficiency. On the other hand, rapamycin showed a distinct pattern, which was, however, partially shared by some interventions (acarbose, GHRKO, Snell dwarf mice, 17-α-estradiol and Protandim). This approach, however, may introduce batch effects resulting from comparison of datasets, which are obtained from the same source and share the same control samples.

To overcome the batch effect and investigate mutual organization of gene expression profiles of longevity interventions at the level of whole transcriptomes, we compared interventions in a pairwise manner, considering only pairs of datasets from different sources. For each of them, we calculated the Spearman correlation coefficient using 250 most significant differentially expressed genes. We then examined the distribution of these correlation coefficients among all pairs of single datasets. We also used the same unbiased procedure to obtain the distribution of correlation coefficients between different datasets related to the same intervention. This let us investigate how persistent gene expression response to certain intervention is across different studies and experimental design settings.

For CR, this method resulted in statistically significant positive correlations with the majority of interventions, including all GH deficient mutants (adjusted Mann-Whitney p-value $< 6.1 \cdot 10^{-10}$), diets, including CR itself (adjusted p-value $= 1.2 \cdot 10^{-95}$), MR and EOD (adjusted p-values $< 1.95 \cdot 10^{-5}$), as well as FGF21 overexpression, acarbose, 17-α-estradiol, metformin and resveratrol (adjusted p-values $< 3.2 \cdot 10^{-3}$) (Fig. 4B). Interestingly, although rapamycin was originally thought to be a CR mimetic, it didn't demonstrate a significant positive correlation with the diet, in accordance with our previous findings (Fig. 3F, 4A) and results of other groups (Fok et al., 2014b; Miller et al., 2014). Instead, the gene expression profile of this drug exhibited a slight but significant negative correlation with CR (median Spearman correlation coefficient = −0.049, adjusted p-value $= 8.9 \cdot 10^{-5}$). The same analysis applied to rapamycin revealed its significant positive correlation only with itself, although even this effect was quite low (median correlation coefficient = 0.088; adjusted p-value = $2.8 \cdot 10^{-3}$) (Fig. S4). This may point to high variability of gene expression responses to rapamycin across experimental settings. It may also be a consequence of higher technical noise due to the generally lower size of the effect for drugs compared to diets and genetic manipulations (Fig. S3A).

Following the same algorithm, we calculated median Spearman correlation coefficients for every pair of interventions calculated across all single datasets (Fig. 4C). We observed a tight cluster formed by GH deficiency and *Fgf21* overexpression. Dietary interventions, including CR, MR and EOD, also showed positive correlation with the mutants and each other. Other interventions exhibited either weak positive correlation with the main cluster (resveratrol, 17-α-estradiol, acarbose, metformin and S6K1 −/−) or distinct gene expression patterns with no significant positive correlations (*Dgat1* −/−, *Myc* +/−, Protandim and rapamycin). To visualize the mutual organization of interventions as a network, we utilized Cytoscape and connected each pair of interventions with significant positive correlation (adjusted p-value < 0.1) (Fig. 4D). In agreement with previous findings (Fig. 4A), most interventions exhibited similarity with CR and GH-deficient mutants. The lack of edges between some of the interventions may be related to insufficient statistics due to low number of independent datasets. The relatively high values of median Spearman correlation for the corresponding interventions (Fig. 4C) suggest that the increase in the number of datasets may fill many edges missing in the network.

Common gene signatures of longevity interventions

We further aimed to discover genes commonly up- or downregulated by longevity interventions that could serve as an approximation of ‘necessary’ features and qualitative predictors of lifespan extension. First, by aggregating profiles across datasets, we identified statistically significant genes related to each intervention. To account for possible differences of the intervention effect on lifespan across doses, ages, strains and sexes introduced by heterogeneity of our data, we only considered datasets, whose experimental conditions were shown to produce statistically significant extension of lifespan.

For every gene, we could then calculate the number of interventions, where it was up- or downregulated (Fig. S5A). One gene (*Gsta4*) was found to be significantly upregulated in 9 different interventions (out of 15) (Fig. S5B) and 7 genes (*Gstt3, Abcb1a, Slc22a29, Slc15a4, Ak4, Serpina6 and Cers6*) were upregulated in 8 interventions (adjusted p-value < 0.1). These genes were involved in xenobiotic (*Gsta4, Gstt3, Abcb1a and Slc22a29*), glucocorticoid (*Serpina6*) and sphingolipid (*Cers6*) metabolism. In addition, 2 genes (*C9* and *C8a*, complement components) were significantly downregulated in 9 and 8 interventions, respectively. However, this approach does not account for difference in the number of datasets associated with every intervention along with difference in quality of the datasets (e.g., number of samples). It also does not consider a level of similarity between interventions at the level of whole transcriptomes, which would make all responses of individual genes similar, regardless of the effect on lifespan.

To overcome these problems, we searched for common signatures using a single mixed-effect model. We utilized a type of intervention as an additional random term and included correlation matrix for this term calculated previously (Fig. 4C). Using this method, we detected only 7 up- and 5 downregulated genes shared by all interventions with adjusted p-value < 0.05 (Table S6A). To detect genes commonly shared by most interventions, we weakened the criteria by letting one intervention to be an outlier. We accomplished this by removing each intervention one by one and taking the best remaining p-value (“robust p-

value" approach). Using the adjusted robust p-value threshold of 0.05, we identified 166 up- and 134 downregulated genes (Fig. 5A).

Interestingly, one of most significant commonly upregulated genes was *Cth* (adjusted robust p-value = 0.0033) (Fig. 5B). *Cth* encodes cystathionine gamma-lyase, which participates in glutathione synthesis and H_2S production (Kabil et al., 2011). H_2S by itself was demonstrated to extend lifespan in worms (Miller and Roth, 2007), and its production increased in response to CR in both sexes in different mouse strains (Mitchell et al., 2016). *Cth* was also shown to be upregulated in response to short-term 50% CR and to mediate oxidative stress resistance under conditions of sulfur amino acid restriction (Hine et al., 2015). Unexpectedly, its expression was increased in response to high-protein diet, which seems to be negatively associated with lifespan (Gokarn et al., 2018). Except for this case, our data suggest that the hepatic expression of *Cth* is increased by most lifespan-extending interventions and could be used as a simple molecular biomarker associated with longevity.

Another interesting example of a commonly upregulated gene is *Brca1* (adjusted p-value = 0.04) (Fig. S6A, Table S6A). This well-known tumor suppressor (Narod and Foulkes, 2004) has also been linked with mouse longevity. In particular, its haploinsufficiency (*Brca1* +/−) led to shortened lifespan (by 8% in mean lifespan) with 70% tumor incidence vs. about 10% in wild-type animals (Cao et al., 2003). Interestingly, besides being related to DNA repair, BRCA1 was shown to physically interact with NRF2 and increase its stability and activation (Gorrini et al., 2013). Consequently, it may act by activating the NRF2-dependent antioxidant response, which is one of shared signatures of longevity interventions (Fig. 3C and 5D).

Several glutathione S-transferase (GST) genes were also significantly upregulated across interventions, including *Gstt2, Gsto1* and *Gsta4* (adjusted robust p-value < 0.037) (Fig. S5B). All of them are involved in glutathione metabolism, known to be activated at the gene expression level in response to CR (Fu and Klaassen, 2014) and several GH deficiency states (Sun et al., 2013; Tsuchiya et al., 2004). Administration of GH was shown to decrease GST activity in several tissues including liver (Brown-Borg et al., 2005). Overall, upregulation of *Gst* genes is a common signature of longevity interventions, and they are significantly changed not only by GH deficiency and CR, but also by FGF21 overexpression, acarbose, MR, MYC deficiency and others (Fig. S5B).

To identify pathways associated with common up- and downregulated gene signatures, we performed functional GSEA (Fig. 5C; Table S4B). In accordance with the RNAseq findings, the most significant upregulated functions included drug metabolism by cytochrome P450 and glutathione metabolism activated by the NRF2 pathway along with ribosome, oxidative phosphorylation, TCA cycle and amino acid metabolism (q-value < 0.075 for all specified functions). Downregulated functions included primary immunodeficiency, RNA polymerase and tRNA metabolic process (q-value < 0.061). Interestingly, several age-related diseases associated at the molecular level with age-dependent changes, such as Alzheimer's, Parkinson's and Huntington's diseases, were enriched for common signatures (q-value < 0.036), pointing to the connection between the changes induced by aging and longevity interventions.

To generalize our findings across tissues, we integrated public data on transcriptomic responses to lifespan-extending interventions for two additional tissues: skeletal muscle and white adipose tissue (WAT) (Table S1D). Using the same method and thresholds, we identified 160 and 390 up- along with 123 and 325 downregulated genes for the muscle and WAT, respectively. Interestingly, there was almost no overlap between discovered genes across different tissues (Fig. 5D). On the other hand, GSEA resulted in the number of shared molecular functions enriched by these signatures (Fig. 5E, Table S4B). Thus, oxidative phosphorylation (q-value < 0.024), amino acid metabolism (q-value < 10^{-3} for liver and WAT), and ribosome structural genes (q-value < 0.061) along with age-related diseases such as Parkinson's and Alzheimer's (q-value < 0.083) were commonly upregulated across tissues, while immune response genes were downregulated (Fig. 5E). Therefore, although longevity interventions seem to affect different individual genes across tissues, these signatures may converge to the same molecular pathways. We also observed some functions being perturbed in a tissue-specific manner, such as drug metabolism by cytochrome P450 activated only in liver.

Signatures associated with the effect on lifespan

To identify genes positively and negatively associated with the degree of lifespan extension, we integrated a previously described mixed-effect regression model with 3 commonly used metrics of lifespan extension obtained from published survival data on corresponding interventions: median lifespan ratio, maximum lifespan ratio and median hazard ratio (the ratio of slopes of survival curves at the timepoint when 50% of cohort is alive). We used these metrics as the most consistent and robust to the effects of sampling size (Moorad et al., 2012). To account for data heterogeneity, we integrated gene expression and longevity data only if they were associated with the same experimental design in terms of sex, strain, dose and the age at which the intervention started.

We designated genes as statistically significant if their adjusted p-value and LOO p-value, obtained after removal of every intervention one by one, were both < 0.05. With these thresholds, we detected 351, 258 and 183 genes with positive and 264, 191 and 108 genes with negative association with maximum lifespan ratio, median lifespan ratio and median hazard ratio, respectively (Fig. 6A and 7D). These gene sets showed a significant overlap (Fisher exact test p-value < 10^{-18} for all pairwise comparisons), which was especially large between median and maximum lifespan. Indeed, 65.1% and 47.9% of genes positively and 52.9% and 38.3% of genes negatively associated with median and maximum lifespan, respectively, were shared across them. One of the strongest positive associations with lifespan was found for *Hint3* (adjusted p-value < $2.5 \cdot 10^{-4}$) encoding nucleotide hydrolase (Fig. 6C). On the other hand, *Irf2* encoding interferon regulatory transcription factor showed a significant negative association with these metrics (adjusted p-value < $1.2 \cdot 10^{-5}$) (Fig. 6D). Other genes positively associated with changes in both maximum and median lifespan included members of fatty acid metabolism (*Acadm, Eci1*) (Fig. 6E), and oxidative phosphorylation pathway (*Atp5f1, Cox17, Ndufb3* and *Ndufab1*) (Fig. 6F).

Interestingly, the fat synthesis enzyme *Dgat1*, whose knockout is associated with extension of mean and maximum lifespan in female mice by 23% and 8%, respectively (Streeper et al.,

2012), was found to have a weak positive association with the effect on lifespan across interventions (slope coefficient = 0.38 and 0.29, adjusted p-value = 0.007 and 0.04 for maximum and median lifespan, respectively) (Fig. 6B). However, the change of *Dgat1* expression appears to be relatively small in response to all interventions, except for *Dgat1* deletion. A similar pattern was observed for *Fgf21*, whose expression was increased only in response to *Fgf21* overexpression. These examples demonstrate that longevity can be achieved through alteration of different master regulators, but these perturbations may result in the same downstream systemic responses, which are related to the lifespan extension effect.

To check if such pattern is universal for different genes, we compared the identified genes shared across signatures and associated with the degree of lifespan effect with the genes whose perturbation was demonstrated to extend mouse lifespan, obtained from GenAge (18 pro- and 38 anti-longevity genes) (De Magalhães and Toussaint, 2004). Indeed, we observed almost no overlap between these gene sets (Fisher exact test p-value > 0.33 for all pairwise comparisons) (Fig. S6B). Therefore, the identified gene signatures appear to reflect the response of the whole molecular system and are associated with longevity when altered together as a group, whereas lifespan-increasing genes represent upstream regulators, whose perturbations, in the end, lead to these systemic changes, similarly to dietary and pharmacological interventions.

To identify pathways enriched by genes positively and negatively associated with the effect on lifespan, we ran GSEA for all 3 metrics of lifespan extension and observed general consistency among them in terms of functional enrichment (Fig. 7C, Table S4C). Thus, genes related to TCA cycle, oxidative phosphorylation, amino acid catabolism and Huntington's and Parkinson's diseases were significantly positively associated among all three metrics used in the analysis (q-value < 0.02 for all specified functions and metrics). On the other hand, regulation of interleukin 1 beta production showed significant negative association with the lifespan metrics (q-value < 0.096 for median lifespan and median hazard ratio) (Fig. 7C). However, some functions, such as peroxisome (q-value = 0.03 for maximum lifespan) and DNA replication (q-value = 0.026 for median hazard ratio), were specific to single lifespan extension metrics.

Some of the hepatic genes and pathways turned out to be both common signatures and signatures associated with the effect on lifespan. In other words, they could be used for prediction of both lifespan extension *per se* (qualitative estimate) and the size of this effect (quantitative estimate). In particular, we identified 26 genes being both commonly changed across interventions and associated with either median or maximum lifespan in the same direction (Table S6B). 17 of them were upregulated and positively associated with effect on lifespan, whereas 9 were downregulated and negatively associated. The identified genes are involved in regulation of apoptosis (*Aatk, Net1, Rb1, Sgms1*), immune response (*C4bp, P2ry14, Slc15a4, Tap2, Rb1*), transcription (*Pir, Sall1*), stress response (*Net1, Nqo1, Pck2, Rb1*), glucose metabolism (*Pck2, Pgm1*) and cellular transport (*Ldlrad3, Slc15a4, Slc25a30* and *Tap2*).

For example, *Nqo1*, encoding NAD(P)H-dependent quinone oxidoreductase involved in oxidative stress response, showed a significant positive association with maximum and median lifespan (adjusted p-value = 0.002 and $7.74 \cdot 10^{-5}$, respectively) and was also commonly upregulated across longevity interventions (adjusted robust p-value = 0.011) (Fig. 7A). Interestingly, this gene is a well-known target of NRF2, an upstream regulator of gene expression changes induced by various lifespan-extending interventions (Leiser and Miller, 2010; Mutter et al., 2015) (Fig. 3C).

Another such gene is *Slc15a4*, which codes for lysosome-based proton-coupled amino acid transporter of histidine and oligopeptides from lysosome to cytosol. In dendritic cells, this protein regulates the immune response by transporting bacterial muramyl dipeptide (MDP) to cytosol and, therefore, activating the NOD2-dependent innate immune response (Nakamura et al., 2014). In addition, its activity affects endolysosomal pH regulation and probably v-ATPase integrity, required for mTOR activation (Kobayashi et al., 2014). Our data show that *Slc15a4* is a common signature of lifespan-extending interventions (adjusted robust p-value = 0.008) along with some other transporters (Fig. 5C) and is positively associated with maximum lifespan (adjusted p-value = 0.02) (Fig. 7B), pointing to the possible importance of lysosomal integrity and amino acid transport for longevity.

At the level of pathways, oxidative phosphorylation showed positive association with both common and lifespan-associated signatures, and some functions involved in liver regulation of the immune response showed negative association (Fig. 5C,E and 7C). Interestingly, downregulation of the electron transport chain was also found by other groups to be the only common signature of aging at the level of gene expression across different species including humans, mice and flies (Zahn et al., 2006). Therefore, contrary to the feminizing effect, this pattern seems to demonstrate the opposite behavior during aging and in response to longevity interventions.

To make our data and tools available to the research community, we developed a web application, GENtervention, based on the R package shiny (Chang et al., 2016). It allows interrogation of gene expression data and, for every gene, it offers (i) expression change across different datasets related to every individual intervention (e.g. Fig. 5B (upper), 7A (upper), 7B (upper), S2, S6B), (ii) expression change in all available datasets across lifespan-extending interventions (common signatures) (Fig. 5B (lower) and S6A), and (iii) the association of expression change with metrics of the longevity effect (signatures associated with the lifespan extension effect) (Fig. 6B-F, 7A (lower) and 7B (lower)). GENtervention may be accessed through the following link: http://gladyshevlab.org/GENtervention/.

Application of longevity signatures for identification of candidate lifespan-extending interventions

In this work, we obtained gene expression signatures associated with the response to well-studied interventions (CR, rapamycin and GH deficiency interventions), as well as gene sets commonly perturbed across different interventions and associated with the effect on lifespan. We considered a possibility that these ‘longevity signatures’ could be used as predictors of new longevity interventions at the gene expression level. We examined this

possibility with two approaches. First, we checked if the signatures could be used to discover association of interventions of interest with the longevity gene expression patterns using publicly available datasets. We also tested their capability to predict new lifespan-extending candidates using Connectivity Map (CMap) (Lamb et al., 2006; Subramanian et al., 2017).

For the first study, we preprocessed 6 publicly available datasets on hepatic gene expression in response to certain *in vivo* interventions in mice, including injection of interleukin 6 (IL-6) (Ramadoss et al., 2010), knockout of methionine adenosyltransferase (*Mat1a*) (Alonso et al., 2017), chronic hypoxia (Baze et al., 2010a), knockout of *Keap1*, an inhibitor of acute stress regulator NRF2 (Osburn et al., 2008), supplementation of SIRT1 activator SRT2104 (Mercken et al., 2014b) and overexpression of the sirtuin *Sirt6* (Kanfi et al., 2012). We then ran a GSEA-based association test using longevity signatures as input subsets (Fig. 7E).

Interleukin-6 (IL-6) is a pro-inflammatory cytokine secreted by T cells and macrophages to support the immune response. It was shown to stimulate the inflammatory and auto-immune response during progression of diabetes (Kristiansen and Mandrup-Poulsen, 2005), Alzheimer's disease (Swardfager et al., 2010), multiple myeloma (Gadó et al., 2000) and others. Moreover, IL-6 was shown to induce insulin resistance directly by inhibiting insulin receptor signal transduction (Senn et al., 2002). We tested if the intraperitoneal injection of IL-6 leads to hepatic gene expression changes associated with longevity signatures. We detected a significant negative association of this intervention with all longevity signatures (adjusted p-value < 0.025) (Fig. 7E), pointing to a potential negative effect of IL-6 on mouse lifespan.

Methionine adenosyltransferase 1A (MAT1A) catalyzes conversion of methionine to S-adenosylmethionine. This enzyme plays a crucial role in methionine and glutathione metabolism. Its activity in liver is increased 205% in Ames dwarf mice compared to wild-type animals (Uthus and Brown-Borg, 2003), and the introduction of GH to these mice led to ~40% decrease in MAT activity in liver (Brown-Borg et al., 2005). Moreover, due to the role of MAT in methionine metabolism, MAT deficiency in liver leads to persistent hypermethioninemia (Ubagai et al., 1995), which may be considered of as the opposite of MR. Therefore, we expected that knockout of *Mat1a* could be negatively associated with longevity signatures. Indeed, our test revealed such a pattern with statistical significance for 4 out of 6 signatures (adjusted p-value < 0.02) (Fig. 7E). Therefore, *Mat1a* knockout seems to induce transcriptomic changes opposite to those caused by longevity interventions and is expected to diminish mouse longevity.

Hypoxia, a reduction in oxygen levels, has suggestive associations with longevity that are not yet well understood. First, aging is associated with hypoxia, e.g. showing 38% reduction in oxygen levels in adipose tissue (Zhang et al., 2011). Second, studies investigating the effect of hypoxia on longevity revealed contrasting results. One group showed that, in *C. elegans,* growth in low oxygen and mutation of VHL-1, a negative regulator of the main modulator of hypoxia HIF-1, extended worm lifespan up to 40% (Mehta et al., 2009). However, another group reported an increased lifespan of *C. elegans* following the deletion

of HIF-1 gene under slightly different conditions (Chen et al., 2009). Also, by generating reactive oxygen species (ROS), hypoxia leads to activation of NRF2, one of the upstream regulators associated with the response to lifespan-extending interventions (Fig. 3C). Finally, hypoxia was found to be among the most effective protectors against mitochondrial disfunction associated with virtually all age-related degenerative diseases (Balaban et al., 2005; Jain et al., 2016). In mammals, chronic hypoxia leads not only to a compensatory increase in oxygen delivery due to increased production and affinity to hemoglobin, decreased weight, higher ventilation rate and capillary density and larger mass of lung, liver and left ventricle (Aaron and Powell, 1993; Baze et al., 2010a), but also to a decrease in demand for oxygen through alteration of metabolism (Gautier, 1996; Steiner and Branco, 2002). To investigate whether chronic hypoxia may induce longevity-associated gene expression patterns, we examined transcriptomes of mice subjected to 11.5 kPa Po_2 hypoxia (11.8% oxygen in the air) for 32 days. We detected a significant positive association of the response to hypoxia with all longevity signatures, except for rapamycin (adjusted p-value < 0.034) (Fig. 7E), suggesting a potential positive effect of this intervention on mouse healthspan and/or lifespan.

NRF2 is one of the key acute stress regulators, which, among others, activates XMEs (Baird and Dinkova-Kostova, 2011) commonly upregulated at the level of hepatic gene expression across longevity interventions (Fig. 5C). Overexpression of the NRF2 ortholog SKN-1 in *C. elegans* leads to a 5-20% increase in average lifespan (Tullet et al., 2008), whereas mutation of its inhibitor, *Keap1*, was shown to increase median lifespan by 8-10% in *Drosophila melanogaster* males (Sykiotis and Bohmann, 2008). Moreover, Protandim, a mixture of 5 botanical extracts known to stimulate NRF2 activation, was proved to increase median lifespan in male mice by 7% (Strong et al., 2016). However, how NRF2 affects longevity of mammals remain unclear. We examined how hepatic gene expression was changed by hepatocyte-specific conditional knockout of *Keap1* in mice and identified statistically significant positive association with almost all longevity signatures, except for rapamycin (adjusted p-value < 0.0015) (Fig. 7E).

We also analyzed the association of sirtuin activation with longevity signatures using two mouse models, SIRT1 activator SRT2104 in males (Mercken et al., 2014b) and *Sirt6* overexpression in both sexes (Kanfi et al., 2012). Both models were shown to extend lifespan of males, but the effect was modest (~10% increase in median and maximum lifespan). Accordingly, we detected significant positive associations for these models in males with CR and common gene patterns. However, there was no consistent positive association with longevity signatures associated with the quantitative effect on lifespan, and we even observed a weak negative association in one of the cases (Fig. 7E). Interestingly, *Sirt6* overexpression in females, which did not affect lifespan during survival studies (Kanfi et al., 2012), also demonstrated no significant associations with longevity signatures (Fig. 7E).

To test if gene expression signatures associated with lifespan extension may be translated across species, we analyzed their association with the hepatic response to CR in rhesus monkeys (*Macaca mulatta*) (Rhoads et al., 2018). We observed a strong significant association with the CR signature, pointing to the existence of shared gene expression

response to this intervention in mammals (Fig. 7E). However, we did not detect an association of CR in monkeys with either common signatures or signatures associated with the effect on lifespan. This may point to a weaker longevity effect of CR in primates or to the different patterns of lifespan extension across species. This may also be due to statistical issues related to a limited sampling size.

Finally, we tested if longevity signatures could be used to predict the difference in lifespan between mouse strains, which may also be considered as genetic intervention. The GSE10421 dataset includes gene expression of male livers from 2 mouse strains tested at the same chronological age (7 weeks old): C57BL/6 and DBA/2 (Kautz et al., 2008). We identified genes with significantly different expression between these strains and subjected them to the association test. All longevity signatures except for rapamycin demonstrated a significant positive association with C57BL/6 gene expression profile compared to that of DBA/2 (adjusted p-value $< 5.3 \cdot 10^{-4}$) (Fig. 7E). Lifespan of C57BL/6 mice (median lifespan = 901 days) is significantly higher than that of DBA/2 (median lifespan = 701 days) (Yuan et al., 2009). This difference was, therefore, captured by the longevity signatures, which were able to identify the strain with greater lifespan. These findings further support the notion that the longevity signatures can be used for the assessment of differences in expected lifespan.

For the second study, to identify candidate lifespan-extending drugs, we utilized the CMap platform (Lamb et al., 2006; Subramanian et al., 2017). It contains gene expression profiles of different human cell lines subjected to > 1,500 compounds and allows searching for perturbagens producing gene expression changes similar to the pattern of interest. To identify drugs with significant longevity effects, we ranked them based on their association with gene signature related to maximum lifespan. We then chose four compounds from the top of the ranking and applied them to UM-HET3 male mice for 1 month (Table S1E). These drugs included two mTOR inhibitors KU-0063794 (García-Martínez et al., 2009) and AZD8055 (Chresta et al., 2010), antioxidant ascorbyl-palmitate (Cort, 1974) and antihypertensive agent rilmenidine (Mpoy et al., 1988).

We performed RNAseq of the liver samples from mice subjected to the drugs, together with the corresponding controls. To check if the hits predicted with human cell lines are reproduced in mouse tissues, we calculated gene expression responses to each of these drugs and passed them to the association test (Fig. 7E). In agreement with the predictions, all compounds demonstrated positive associations with the common gene signature across lifespan-extending interventions (adjusted p-value < 0.077). Moreover, KU-0063794 and ascorbyl-palmitate showed a consistent positive association with all longevity signatures, except for rapamycin (adjusted p-value < 0.055). AZD8055 and rilmenidine also showed a positive association with some of the signatures, including CR and GH deficiency, but not with the gene sets associated with the effect on lifespan. This inconsistency may be due to imperfect translation of gene expression responses from human cell lines to mouse *in vivo* models or insufficient sampling size. Yet, in general, this pilot study demonstrates applicability of this approach for the identification of new interventions with a desirable effect on gene expression and offers appealing candidates for further studies.

CONCLUSIONS

We collected and characterized RNAseq data on several lifespan-extending interventions, including three that had never been analyzed at the level of gene expression, across sexes, doses and age groups. We observed a significant feminizing pattern of gene expression changes in males in response to genetic and dietary interventions at both transcriptomic and metabolomic levels. This effect was associated with perturbations of common genes and molecular pathways including those regulated by GH. The feminizing effect couldn't explain lifespan extension but was associated with the diminution of sex-associated differences pointing to the converging effect of lifespan-extending interventions on hepatic transcriptome and metabolome across sexes.

Expanding this analysis with available microarray data allowed us to define gene expression signatures associated with individual interventions (rapamycin, CR and GH deficiency) as well as shared across longevity interventions. We observed that, despite some differences, most of them perturb similar genes and pathways, including upregulation of XMEs regulated by NRF2, TCA cycle, oxidative phosphorylation, and ribosome protein genes, and downregulation of complement and coagulation cascades. Many of these functions turned out to be affected across tissues. Moreover, some genes involved in stress response, apoptosis, glucose metabolism, and immune response, as well as certain pathways, such as oxidative phosphorylation, were found to be commonly perturbed across interventions and, at the same time, associated with the effect on lifespan, serving as both qualitative and quantitative predictors of lifespan extension. These genes and processes seem to be the most persistent and reliable determinants of longevity in mice and deserve further exploration. We further developed a publicly available web application GENtervention that can be used to interrogate this dataset.

Finally, we employed gene expression signatures to identify new lifespan-extending interventions based on gene expression data. Here, our algorithm could distinguish two mouse strains of the same age with different expected lifespans. We have also found that hypoxia and hepatocyte-specific *Keap1* knockout are positively associated with longevity signatures at the level of gene expression and, therefore, appear to be strong candidates for experimental validation. In addition, we demonstrated applicability of this method to predict new candidate lifespan-extending compounds using CMap and validated the detected positive association of gene expression profile induced by KU-0063794 and ascorbyl-palmitate, making them appealing candidates for further investigation and survival studies.

Limitations of study

Compared to previous research that focused on the effects of single or a small number of lifespan-extending interventions, the current study aggregated transcriptomic responses across a wide range of interventions that were applied to different strains, sexes and age groups. Although such heterogeneity of experimental design appears to be a crucial advantage supporting robustness of the identified patterns, it is associated with variability of gene expression responses. This may, in turn, result in the decreased statistical power and complicate direct comparison of interventions. It should also be noted that the compounds predicted by CMap are based on the comparison of mouse *in vivo* longevity patterns and

responses in human cell lines, and this may introduce bias related to differences across biological models and species. Therefore, gene expression responses to drugs identified with such approach should be validated in mouse tissues, as demonstrated in our work. In addition, the effect of candidate interventions on lifespan needs to be experimentally confirmed in survival studies or tested with biomarkers of aging before they can be designated as lifespan-extending interventions. Despite these potential limitations, we believe that the approach developed in this work will greatly facilitate a search for new interventions and help screen candidate genes and drugs prior to costly lifespan analyses.

STAR METHODS

LEAD CONTACT AND MATERIALS AVAILABILITY

Further information and requests for resources and reagents should be directed to and will be fulfilled by the Lead Contact, Vadim N. Gladyshev (vgladyshev@rics.bwh.harvard.edu). This study did not generate new unique reagents.

EXPERIMENTAL MODEL AND SUBJECT DETAILS

Animals and Methionine Restriction—Mice were subjected for methionine restriction (MR) as described in (Ables et al., 2012, 2015). Seven-weeks old male C57BL/6J mice were purchased from The Jackson Laboratory (Stock #000664, Bar Harbor, ME, USA) and housed in a conventional animal facility maintained at 20 ± 2°C and 50 ± 10% relative humidity with a 12 h light: 12 h dark photoperiod. During a 1-week acclimatization, mice were fed Purina Lab Chow #5001 (St. Louis, MO, USA). Mice were then weight matched and fed either a control (CF; 0.86% w/w methionine) or MR (0.12% w/w methionine) diet consisting of 14% kcal protein, 76% kcal carbohydrate, and 10% kcal fat (Research Diets, New Brunswick, NJ, USA) for 52 weeks. Body weight and food consumption were monitored twice weekly. Young mice were 8 weeks old (2 months) at the initiation of the experiments and 60 weeks old (14 months) upon termination. On the day of sacrifice, animals were fasted for 4 hours at the beginning of the light cycle. After mice were sacrificed by CO_2 asphyxiation, liver samples were collected, flash frozen, and stored at −80°C until analyzed. All experiments were approved by the Institutional Animal Care and Use Committee of the Orentreich Foundation for the Advancement of Science, Inc. (Permit Number: 0511MB).

Animals and Lifespan-Extending Interventions—Other mice used in this study were obtained from the colonies at University of Michigan Medical School and subjected to interventions as described in (Harrison et al., 2014; Miller et al., 2011, 2014; Strong et al., 2016). Liver samples corresponding to lifespan-extending interventions for RNA-seq and metabolome analysis were taken at 6 and 12 months of age from male and female mice treated by drugs or exposed to caloric restriction (CR) diet from 4 months of age along with control mice, which were untreated littermate mice matched by age and sex. The design of experiment was in accordance with intervention testing program (ITP) studies, which confirmed the lifespan-extending effect of these interventions. Interventions analyzed at 6 months of age included 40% CR, Protandim™ (1,200 ppm, as in (Strong et al., 2016)), rapamycin (42 ppm, as in (Miller et al., 2014)), 17-a-estradiol (14.4 ppm, as in (Strong et al.,

2016)) and acarbose (1000 ppm, as in (Harrison et al., 2014)), while interventions analyzed at 12 months of age included 40% CR, acarbose (1000 ppm, as in (Harrison et al., 2014)) and rapamycin (14 ppm, as in (Miller et al., 2011, 2014)). All organisms received the same diet (Purina 5LG6) made in the same commercial diet kitchen (TestDiet, Richmond, IN, USA). All mice, except for those subjected to CR, were fed *ad libitum*. Genetically heterogenous UM-HET3 strain, in which each mouse had unique genetic background but shared the same set of inbred grandparents (C57BL/6J, BALB/cByJ, C3H/HeJ, and DBA/2J), was used in this setting. This cross produces a set of genetically diverse animals, which minimizes the possibility that the identified signatures represent gene expression patterns specific to inbred lines. Moreover, this strain was used by ITP to test the lifespan extension potential of the compounds analyzed in this study. In all cases, interventions continued until the animals were sacrificed.

Liver samples from Snell dwarf (Flurkey et al., 2001) and GHRKO (Coschigano et al., 2003) males, and their sex- and age-matched littermate controls, were taken from mice at 5 months of age belonging to (PW/J × C3H/HeJ)/F2 and (C57BL/6J × BALB/cByJ)/F2 strains, respectively.

All mice were kept at a density of 3 males or 4 females per ventilated cage, in a specific-pathogen free vivarium, with 12:12 light:dark cycle. Animals were moved to fresh cages every 14 days. Maintenance of specific-pathogen free status was documented quarterly, using sentinel mice exposed to spent bedding sampled from each experimental cage, and evaluated by a mixture of fecal RT-PCR tests and serology for anti-viral antibodies. Health was evaluated daily for each mouse. Veterinary oversight was provided by faculty and residents of the Unit for Laboratory Animal Medicine, and all protocols were approved by the University of Michigan's Institutional Animal Care and Use Committee.

Animals and Compounds with Predicted Effect—3-month old UM-HET3 mice were obtained from the colonies at University of Michigan Medical School and subjected to diets containing compounds predicted with the longevity gene expression signatures via Connectivity Map (CMap): KU-0063794 (10 ppm, as in (Yongxi et al., 2015)), AZD8055 (20 ppm, as in (García-Martínez et al., 2011)), ascorbyl-palmitate (6.3 ppm, as in (Veurink et al., 2003)) and rilmenidine (10 ppm, as in (Jackson et al., 2014)) for 1 month. Liver samples were taken from treated mice along with their untreated sex- and age-matched littermates, which were fed *ad libitum.* In all cases, interventions continued until the animals were sacrificed. All animal protocols were approved by the Institutional Animal Care and Use Committee. Housing conditions were identical to those described previously.

METHOD DETAILS

Gene Expression Profiling of Liver Tissues—For RNA-seq analysis corresponding to lifespan-extending interventions, 3 biological replicates were used for each experimental group, including both treated and control mice, resulting in the total of 78 samples (Table S1A). For RNA-seq analysis corresponding to drugs predicted with longevity signatures, we used 4 and 8 biological replicates per experimental group for treated and control mice,

respectively, resulting in the total of 24 samples (Table S1E). RNA was extracted from liver tissues with PureLink RNA Mini Kit as described in the protocol and passed to sequencing.

For samples corresponding to lifespan-extending interventions, paired-end sequencing with 100 bp read length was performed on Illumina NovaSeq 6000 platform. For samples corresponding to predicted compounds, libraries were prepared as described in (Hashimshony et al., 2016) and sequenced with 100 bp read length option on the Illumina HiSeq 2500.

Metabolite Profiling of Liver Tissues—Metabolite profiling of male and female UMHET-3 mice subjected to control diet, acarbose and rapamycin (Data S1A) was performed using four complimentary liquid chromatography-mass spectrometry (LC-MS) methods, including HILIC analysis of water soluble metabolites in the positive ionization mode (HILIC-pos), HILIC analysis of water soluble metabolites in the negative ionization mode (HILIC-neg), positive ion mode analysis of polar and non-polar plasma lipids (C8-pos) and negative ion mode analysis of free fatty acids and bile acids (C18-neg), as in (Paynter et al., 2018). We utilized at least 5 and 8 biological replicates per experimental group for treated and control mice, respectively, resulting in the total of 39 samples (Table S1B). The samples were homogenates of freshly frozen tissues of sacrificed animals, matched by age and sex.

Raw data from Q Exactive/Exactive Plus instruments were processed using TraceFinder software (Thermo Fisher Scientific; Waltham, MA) and Progenesis QI (Nonlinear Dynamics; Newcastle upon Tyne, UK) while MultiQuant (SCIEX; Framingham, MA) was used to process 5500 QTRAP data. For each method, metabolite identities were confirmed using authentic reference standards or reference samples.

QUANTIFICATION AND STATISTICAL ANALYSIS

RNAseq Data Processing and Analysis—Quality filtering and adapter removal were performed using Trimmomatic (version 0.32) (Bolger et al., 2014). Processed/cleaned reads were then mapped with STAR (version 2.5.2b) (Dobin et al., 2013) and counted via featureCounts (version 1.5) (Liao et al., 2014). To filter out genes with low number of reads, we left only genes with at least 6 reads in at least 66.6% of samples, which resulted in 12,861 and 8,999 detected genes according to Entrez annotation for RNAseq corresponding to lifespan-extending interventions and compounds predicted by CMap, respectively. Filtered data was then passed to RLE normalization (Anders and Huber, 2010).

Differential expression analysis was performed with R package edgeR (Robinson et al., 2009). For individual interventions, we declared gene expression to be significantly changed, if p-value, adjusted by Benjamini-Hochberg procedure (Benjamini and Hochberg, 1995), was smaller than 0.05 and fold change (FC) was bigger than 1.5 in any direction. When several doses and age groups were presented, we added separate factors accounting for that to the model and looked for genes significantly changed across these settings. As dose and age groups experiments were run separately and had their own controls, such factors allowed us to adjust for possible batch effect. The effects of certain interventions on different sexes were investigated separately. To determine the statistical significance of overlap between

differentially expressed genes corresponding to certain interventions, we performed Fisher exact test separately for up- and downregulated genes, considering 12,861 detected genes as a background.

When performing analysis of the feminizing effect, gene expression differences were identified between control males and females from UM-HET3 strains for each age group. Gene was declared significant if p-value, adjusted by Benjamini-Hochberg procedure, was smaller than 0.05 and FC was bigger than 1.5 in any direction. Identified lists of genes are stored in Table S3A. The intersection of these gene sets was used for subsequent calculation of the feminizing effect and distances between sexes. The statistical significance of correlation between sex-associated differences and response to certain intervention ("feminizing effect") was calculated using Spearman correlation test and adjusted for multiple comparisons with Benjamini-Hochberg procedure. When calculating correlation between response to certain intervention in specific age group (6 or 12 months) and female-associated differences, the latter were calculated using gene expression data for control males and females from the other age group (12 or 6 months, respectively). This approach provided us with unbiased correlations, based on different control samples and, therefore, free of regression to the mean effect. In case of MR, GHRKO and Snell dwarf mice, which possess their own controls, the feminizing effect was calculated using both age groups. Feminizing effect calculations are shown in Table S3C.

Differences in the feminizing effect of interventions in certain age groups between males and females were tested by Spearman correlation test, applied to the difference in $\log_2$FC of gender-associated genes in response to the specified conditions between males and females, and female-associated differences based on the other age group, with the following Benjamini-Hochberg adjustment. Manhattan distance between male and female gene expression profiles was calculated for individual samples in a pairwise manner using intersection of sex-specific gene sets across age groups. Unpaired Mann-Whitney test and Benjamini-Hochberg adjustment were used to assess statistical significance of difference between gender gene expression distances of control mice and animals subjected to interventions. Overlap between statistically significant sex-associated genes and genes differentially expressed in response to interventions was estimated by Fisher exact test similarly to comparison of individual interventions.

Heatmap of feminizing genes was created based on feminizing changes, aggregated across age groups, and $\log_2$FC of corresponding genes in response to individual interventions, aggregated across age groups as well (using edgeR). Only genes differentially expressed between control males and females (637 genes) were used to build the heatmap. Clustering was performed with average hierarchical approach and Spearman correlation distance.

To investigate genes responsible for the feminizing effect, we used single edgeR model to identify genes with changes associated with the feminizing effect, calculated within unbiased correlation analysis. We declared a gene to be significantly changed, if its Benjamini-Hochberg adjusted p-value was smaller than 0.05. We then took an intersection of sex-associated genes, aggregated across age groups, and genes associated with the

feminizing effect, separately for up- and downregulated genes, to obtain the final list of common genes. This resulted in 164 upregulated and 153 downregulated genes.

Metabolome Data Processing and Analysis—To filter out metabolites with low coverage, only metabolites detected in at least 66.6% of the samples were remained. Afterwards, filtered data were log10-transformed and scaled (Data S1B). The data were further aggregated with our previous metabolome dataset on acarbose, rapamycin, CR, GHRKO and Snell dwarf mice models together with the corresponding controls, obtained using similar experimental procedure (Ma et al., 2015). The second dataset was preprocessed in the same way as the first one. Genetic background, age groups and treatment doses in both datasets were consistent with those used for gene expression analysis (Table S1B).

Analysis of the feminizing effect was performed similarly to that described for gene expression. First, metabolites that differ between control males and females were identified for each dataset using limma. Metabolite was declared significant if p-value, adjusted by Benjamini-Hochberg procedure, was less than 0.1. The identified lists of metabolites are shown in Table S3B. Then, statistical significance of the feminizing effect was calculated using Spearman correlation test and adjusted for multiple comparisons with Benjamini-Hochberg. For unbiased analysis, when calculating correlation between the response to certain interventions in specific datasets (new or published one) and female-associated differences, the latter were used from the metabolite data corresponding to the other dataset (the published or the new one, respectively) together with the set of metabolites identified for that dataset. In the case of GHRKO and Snell dwarf mice, which had their own controls, the feminizing effect was calculated using both datasets. The findings involving feminizing effect calculations are shown in Table S3C.

Differences in the feminizing effect of certain interventions in certain datasets between males and females was tested by Spearman correlation test, applied to the difference in $\log_2$FC of gender-associated metabolites (identified based on the other dataset) in response to the specified conditions between males and females, and female-associated differences from the other dataset, with the following Benjamini-Hochberg adjustment. Manhattan distance between male and female metabolite profiles was calculated for individual samples in a pairwise manner using intersection of sex-specific metabolite sets across datasets. Unpaired Mann-Whitney test and Benjamini-Hochberg adjustment were used to assess statistical significance of difference between gender-associated metabolite profile distances of control mice and animals subjected to interventions.

Functional Enrichment Analysis—For identification of functions enriched by genes differentially expressed in response to individual interventions within our RNAseq data and aggregated across datasets (CR, rapamycin and GH deficiency interventions), commonly changed across interventions (common signatures) as well as associated with the effect on lifespan, we performed gene set enrichment analysis (GSEA) (Subramanian et al., 2005) on a pre-ranked list of genes based on $\log_{10}$(p-value) corrected by the sign of regulation, calculated as:

$$-log_{10}(pv) \times sgn(lfc),$$

where *pv* and *lfc* are p-value and logFC of certain gene, respectively, obtained from edgeR output, and *sgn* is signum function (is equal to 1, −1 and 0 if value is positive, negative and equal to 0, respectively). REACTOME, BIOCARTA, KEGG and GO biological process and molecular function from Molecular Signature Database (MSigDB) have been used as gene sets for GSEA (Subramanian et al., 2005). q-value cutoff of 0.1 was used to select statistically significant functions. Significance scores of enriched functions were calculated as:

$$significance\ score = -log_{10}(qv) \times sgn(NES),$$

where *NES* and *qv* are normalized enrichment score and q-value, respectively.

Horizontal and vertical barplots were shown for manually chosen statistically significant functions with size of barplot being dependent on value of significance score. For functions associated with the lifespan effect and common signatures across tissues, heatmap colored based on significance scores was used. Clustering of functions enriched by individual interventions within RNAseq data was performed based on NES of functions with statistically significant enrichment (q-value < 0.1) by at least one intervention. Clustering has been performed with hierarchical average approach and Spearman correlation distance.

To identify functions enriched by genes shared by differences between males and females along with changes in response to lifespan-extending interventions in males, we performed Fisher exact test using Database for Annotation, Visualization and Integrated Discovery (DAVID) (Huang et al., 2009a, 2009b). INTERPRO, KEGG and GO BP and MF databases were used. We declared functions to be enriched if their Benjamini-Hochberg adjusted Fisher exact test p-value was smaller than 0.1.

Aggregation of Datasets for Meta-Analysis—To identify signatures associated with lifespan extension and the effect of certain interventions, we expanded our data with publicly available datasets from Gene Expression Omnibus (GEO) (Edgar, 2002) and ArrayExpress (Kolesnikov et al., 2015) databases: E-MEXP-153 (Amador-Noguez et al., 2004), E-MEXP-2320 (Selman et al., 2009), E-MEXP-347 (Amador-Noguez et al., 2005), E-MEXP-748 (Selman et al., 2006), GSE1093 (Tsuchiya et al., 2004), GSE11845 (Pearson et al., 2008), GSE2431 (Dhahbi et al., 2005), GSE26267 (Streeper et al., 2012), GSE3129 (Boylston et al., 2006), GSE3150 (Boylston et al., 2006), GSE36838 (Zhou et al., 2012), GSE39313 (Zhang et al., 2012), GSE40936 (Martin-Montalvo et al., 2013), GSE40977 (Fok et al., 2014b), GSE46895 (Mercken et al., 2014a), GSE48331 (Fok et al., 2014a), GSE48333 (Fok et al., 2014a), GSE50789 (Collino et al., 2013), GSE51108 (Sun et al., 2013), GSE55272 (Hofmann et al., 2015), GSE61233 (Rusli et al., 2015), GSE6323 (Edwards et al., 2007), GSE70857, GSE81959 (Mitchell et al., 2016) and GSE988 (Rowland et al., 2005). For the analysis of signatures associated with certain interventions (CR, rapamycin, GH deficiency), we integrated available gene expression data obtained from liver of mice

from healthy genetic strains on standard diets subjected to CR, rapamycin and mutations associated with GH deficiency (Ames dwarf mice, GHRKO, Little mice, Snell dwarf mice). For the analysis of signatures shared across lifespan-extending interventions, we included only the data with the experimental design statistically confirmed to extend lifespan. Finally, for the analysis of signatures associated with the lifespan extension effect, we integrated datasets on interventions with available and reliable survival data corresponding to the same experimental design (sex, strain, dose, age when the intervention started). In total, our hepatic meta-analysis covered 17 different interventions presented in 77 control-intervention datasets from 22 different sources (including ours) (Fig. 3D, Table S1). The same approach was used to obtain microarray data corresponding to white adipose tissue (WAT) (9 control-intervention datasets from 5 sources: GSE60596 (Soo et al., 2015), GSE70857, GSE75574 (Barger et al., 2017), GSE39313 (Zhang et al., 2012) and GSE55272 (Hofmann et al., 2015)) and skeletal muscle (13 control-intervention datasets from 9 sources: GSE11291 (Barger et al., 2008), GSE11845 (Pearson et al., 2008), GSE39313 (Zhang et al., 2012), GSE40936 (Martin-Montalvo et al., 2013), GSE49000 (Mercken et al., 2014b), GSE55272 (Hofmann et al., 2015), GSE6323 (Edwards et al., 2007), GSE70857 and GSE75574 (Barger et al., 2017)) (Table S1D).

To aggregate data across different platforms and studies, we developed the following method. First, data within each study was preprocessed independently and log-transformed to conform to normal distribution if needed. Then, filtering of low-covered genes was performed with soft threshold. Then, all identifiers were mapped to Entrez ID gene format, and genes not detected in our RNAseq data were filtered out. This resulted in the coverage of 12,861 genes or less if some of these genes were filtered out because of the low coverage. Afterwards, samples within every study were normalized by quantile normalization and scaling, followed by multiplication by the certain value to make it on the same scale as RNAseq data with more natural interpretation. Finally, mean and standard error of logFC of every gene for every response to intervention was calculated together with p-value (along with Benjamini-Hochberg adjusted p-value) estimated by edgeR (Robinson et al., 2009) and limma (Ritchie et al., 2015) for RNAseq and microarrays datasets, respectively. This resulted in 2 values representing every gene from every dataset. Importantly, one study may include several datasets if several interventions or settings have been analyzed there, and sometimes, different interventions or doses share the same control samples. This may be a source of batch effect, which we removed during subsequent steps of the analysis.

Scaling of genes within every sample, performed before calculation of logFC, results in similar and comparable distribution of gene changes across different studies and platforms. Importantly, scaling is not performed after calculation of logFC as different interventions may lead to different size of gene expression profile perturbation. Indeed, lifespan-extending genetic manipulations generally lead to bigger perturbation of transcriptome compared to diets and compounds (Fig. S1). To demonstrate this effect, we calculated median and standard deviation of logFC distribution across the whole transcriptome for every individual dataset. Median may be interpreted as imbalance between up- and downregulated changes whereas standard deviation corresponds to the scale of perturbation. To visualize distribution of specified metrics for different kinds of interventions (pharmacological, dietary and genetic manipulations), we used violinplots. Unpaired Mann-Whitney test was used to

compare medians and standard deviations of logFC distributions corresponding to different kinds of interventions.

Gene Signatures of Individual Interventions—logFC calculated for every dataset were further used as inputs to the statistical tests for meta-analysis. To account for standard error of logFC and remove batch effect related to the belonging of several datasets to the same study or same control sampling within the study, we applied mixed-effect model using R package metafor (Viechtbauer, 2010). As an input, we used both mean and standard error of logFC. Such approach allowed us to account for the size of the effect and variance of estimated gene expression change within each individual dataset, which provides a more sensitive and accurate analysis compared to previous studies focused on the comparison of lists of differentially expressed genes.

When calculating gene expression changes of individual interventions across different sources (such as CR and rapamycin), to remove batch effect, belonging to the same study or control group was considered as a random term. When calculating such changes for GH deficiency interventions, we also included type of intervention as a random term. Using this procedure, we obtained aggregated logFC and corresponding p-value for every gene. Besides standard p-value, we also calculated leave-one-out (LOO) and robust p-value. ‘LOO p-value’ is defined as the highest p-value after removal of every study one by one. On the other hand, ‘robust p-value’ is the lowest p-value after the same procedure. Benjamini-Hochberg procedure was used to adjust every type of p-value for multiple comparisons. We declared genes to be differentially expressed in response to CR, rapamycin and GH deficiency across datasets if adjusted p-value was smaller than 0.01 and their LOO p-value was smaller than 0.01. The significance of overlap between the lists of differentially expressed genes obtained from meta-analysis was estimated by Fisher exact test separately for up- and downregulated genes, considering 12,861 detected genes as background.

Similarly, aggregated logFC together with p-values were calculated for all interventions presented in our data by multiple sources. For interventions presented as a single dataset, logFC and p-values were obtained from individual datasets as described previously. For interventions measured in several datasets from the same source, single edgeR or limma model was used depending on the origin of the data (RNAseq or microarray). This resulted in the matrix containing aggregated $\log_2$FC values of every gene in response to different interventions. To visualize change of each gene within each individual intervention, we built barplots representing aggregated log2FC of a certain gene in response to all intervention where it has been detected. Statistically significant changes were defined based on Benjamini-Hochberg adjusted p-value.

To identify upstream regulators of the detected gene expression response to CR, rapamycin and GH deficiency, we applied the TRANSFAC platform (Matys, 2006). First, for every individual dataset, we identified transcription factor binding to sequences enriched in the promoters of differentially expressed genes using the platform. This resulted in a matrix, where every transcription factor was either enriched (1) or not (0) for the certain dataset. At this step, we excluded redundant IDs corresponding to different binding patterns of the same factor by considering factor to be enriched if at least one of its patterns is enriched. This

resulted in 1,466 different upstream regulators. To identify factors overrepresented across different datasets of the same intervention, we applied permutation version of binomial statistical test as described in (Plank et al., 2012). Briefly, to identify the p-value threshold corresponding to the desired FDR (equal to 0.01), permutation test is performed, where 1 and 0 (corresponding to enrichment of different transcription factors) are shuffled within each dataset and number of false positives for different binomial test p-value thresholds are calculated. Based on the obtained numbers, p-value threshold ensuring FDR threshold of 0.01 is determined. The significance of overlap between enriched upstream regulators of different interventions was estimated by Fisher exact test, considering 1,466 non-redundant transcription factors as background.

Mutual Organization of Interventions—To assess similarity of gene expression response across interventions, we built a heatmap of aggregated $\log_2$FC of genes significantly changed in response to CR, rapamycin and GH deficiency interventions (2507 genes in total). Complete hierarchical clustering was employed for the heatmap. Correlation matrix representing similarity between aggregated logFC of different interventions was calculated based on Spearman correlation coefficient.

To calculate correlations between interventions in unbiased way, we applied the following approach. For every pair of interventions, including comparison of intervention with itself, we examined all pairs of datasets from different sources. For each such pair we selected 250 genes consisting of 125 genes with the most significant expression change (with the lowest p-values) from each dataset and calculated Spearman correlation coefficient within the pair. We reiterated this algorithm and, as a result, for every pair of interventions obtained distribution of Spearman correlation coefficients, calculated between datasets from different sources. For CR and rapamycin, we visualized these distributions using violinplot. One-sample Mann-Whitney test and Benjamini-Hochberg adjustment were used to check if means of correlation coefficients are different from 0 with statistical significance. We declared correlation coefficient to be significant if adjusted p-value was smaller than 0.1.

For correlation matrix we employed median values of Spearman correlation coefficients. By filtering out comparisons of datasets from the same source, we removed possible batch effect and ended up with independent and unbiased comparison of interventions. However, as some interventions were presented only within the same source, we couldn’t estimate unbiased correlation for such cases. This missing data was visualized by grey boxes. The same was sometimes true for comparison of intervention with itself, as in this case we also employed only datasets from different sources. For this reason, correlation coefficient of intervention with itself was not equal to 1 in resulted unbiased correlation matrix. Complete hierarchical clustering approach was employed for visualization of correlation matrix.

To demonstrate similarities between different interventions in network mode, we employed Cytoscape (Shannon et al., 2003). Only edges between interventions with significant positive correlation coefficients (median Spearman correlation coefficient > 0 and adjusted Mann-Whitney p-value < 0.1) were shown. The width of edge was defined by the $\log_{10}$(adjusted p-value). Smaller p-value led to wider edge.

Gene Signatures of Lifespan Extension—To identify hepatic genes, whose expression change is shared across lifespan-extending interventions, we filtered out all interventions and settings with unproven lifespan extension effects. To account for possible differences in the intervention effect on lifespan across different sexes, ages, strains and doses, we only considered the datasets, whose experimental settings were shown to produce a statistically significant extension of lifespan. Therefore, for example, 40% CR in C57BL/6 females was excluded from the analysis as this setting doesn't lead to a statistically significant lifespan extension, contrary to 20% CR applied to the same mouse strain (Mitchell et al., 2016). In the case of drugs, we also filtered out the datasets containing the response to compounds, which had not been confirmed by ITP studies (such as metformin and resveratrol).

First, for every single gene we calculated number of interventions, where it is differentially expressed based on adjusted aggregated p-value estimated as described previously. We considered gene to be differentially expressed if its adjusted aggregated p-value was smaller than 0.1. However, this approach overfits genes changed in response to similar interventions (such as GH deficiency interventions) and doesn't take into account possible consistent changes, which may be, however, not significant due to low sampling size or high variance. To overcome this problem, we applied single mixed-effect model to every gene as described previously and looked for genes, whose aggregated logFC across lifespan-extending interventions is significantly different from 0. Here, however, we also included the type of intervention as a random term together with correlation matrix specifying similarities between general response of the interventions. This correlation matrix was taken from unbiased mutual organization analysis described previously. We declared genes to be significantly shared across interventions if Benjamini-Hochberg adjusted robust p-value, obtained after removal of every type of intervention one by one, was smaller than 0.05. The same approach was used to identify genes shared across lifespan-extending interventions in the skeletal muscle and WAT. Heatmap with expression changes of significant genes across individual datasets was clustered using a complete hierarchical approach.

To identify genes associated with the lifespan effect, first, we estimated three main metrics of lifespan for every available setting, including median lifespan ratio (in logarithmic scale), maximum lifespan ratio (in logarithmic scale), defined as ratio of average lifespan of 10% most survived individuals, and median hazard ratio, defined as ratio of slopes of survival curves at the median point (timepoint where 50% of cohort is remained survived). These metrics were obtained from published survival data for the corresponding interventions. To account for heterogeneity of our data, we integrated gene expression and longevity studies only if they were associated with the same experimental design (sex, dose, strain, age when intervention started). We then calculated average metric values across the studies to obtain most consistent and reliable estimates. Interventions or settings, for which no appropriate longevity study was available, were excluded.

Afterwards, we applied mixed-effect model as described previously to identify genes associated with each of the 3 numeric metrics of the lifespan effect. Control group and type of intervention were considered as random term, and correlation matrix between interventions was used to define covariance matrix. We declared genes to be significantly

associated with the lifespan effect if Benjamini-Hochberg adjusted p-value and LOO p-value, obtained after removal of every intervention one by one, were both smaller than 0.05. The significance of overlap between lists of genes associated with different metrics of the lifespan effect was estimated by Fisher exact test separately for genes with positive and negative association, considering 12,861 detected genes as a background. Complete hierarchical clustering was used to sort genes on heatmap, representing logFC of genes with significant association across individual datasets. Individual datasets were sorted there based on their effect on maximum lifespan.

Overlap between gene signatures associated with lifespan extension and genes, whose manipulation was demonstrated to extend or shorten mouse lifespan, was estimated by Fisher exact test, as described previously. The latter set was obtained from GenAge database and included 84 and 44 genes with pro- and anti-longevity effects, respectively (De Magalhães and Toussaint, 2004).

Prediction of Lifespan-Extending Effects—To test association of interventions with longevity signatures related to individual interventions (CR, rapamycin and GH deficiency), common changes and lifespan effect association, we employed GSEA-based approach. First, for every signature we specified 250 genes with the lowest p-values and divided them into up- and downregulated genes. These lists were considered as gene sets. Then we ranked genes related to interventions of interest based on their p-values, calculated as described in functional enrichment section. When running association test for lifespan-extending interventions (Fig. 4A), we used p-values obtained from the aggregated analysis as described earlier.

For interventions from publicly available sources (Fig. 7E (upper)), we downloaded them from GEO under the following accession numbers: GSE21060 (Ramadoss et al., 2010), GSE77082 (Alonso et al., 2017), GSE15891 (Baze et al., 2010b), GSE11287 (Osburn et al., 2008), GSE49000 (Mercken et al., 2014b), GSE10421 (Kautz et al., 2008) and GSE104234 (Rhoads et al., 2018). Data corresponding to *Sirt6* overexpression (Kanfi et al., 2012) were downloaded via the link provided in the original paper. When running association test for the rhesus monkey data, we converted monkey genes to mouse orthologs using Ensembl BioMart platform. We preprocessed each dataset, performed quantile normalization and Entrez ID transformation and applied limma model for calculation of p-values, which were converted to $\log_{10}$(p-value) corrected by the sign of regulation as explained earlier.

For compounds predicted with the longevity signatures via CMap, we calculated p-values of gene expression changes compared to control independently for every drug using edgeR. We then converted them to $\log_{10}$(p-value) corrected by the sign of regulation as described earlier and proceeded to GSEA-based analysis.

We calculated GSEA scores separately for up- and downregulated lists of gene set as described in (Lamb et al., 2006) and defined final GSEA score as a mean of the two. To calculate statistical significance of obtained GSEA score, we performed permutation test where we randomly assigned genes to the lists of gene set maintaining their size. To get p-value of association between certain intervention and longevity signature, we calculated the

frequency of real final GSEA score being bigger by absolute value than random final GSEA scores obtained as results of 3,000 permutations. To adjust for multiple comparisons, we performed Benjamini-Hochberg procedure. Resulted adjusted p-values were converted into significance scores as:

$$significance\ score = -\log_{10}(adj.\ pv) \times sgn(GSEA\ score),$$

where *adj. pv* and *GSEA score* are BH adjusted p-value and final GSEA score, respectively. Heatmaps were colored based on values of significance scores.

DATA AND CODE AVAILABILITY

RNAseq data are available at Gene Expression Omnibus (GEO) (Edgar, 2002) under accession number GSE131901 (SubSeries GSE131754 and GSE131868).

Metabolome data are stored in Data S1.

GENtervention App is available via the following link: http://gladyshevlab.org/GENtervention/.

Supplementary Material

Refer to Web version on PubMed Central for supplementary material.

ACKNOWLEDGMENTS

We would like to thank Margarita Meer for discussion and assistance with experimental procedures and Ilia Kurochkin for help with graphical software. Supported by NIH grants AG047745, AG021518, AG047200, and GM065204, and the Russian Federation grant 14.W03.31.0012.

REFERENCES

Aaron EA, and Powell FL (1993). Effect of chronic hypoxia on hypoxic ventilatory response in awake rats. J. Appl. Physiol 74, 1635–1640. [PubMed: 8514677]

Ables GP, Perrone CE, Orentreich D, and Orentreich N (2012). Methionine-Restricted C57BL/6J Mice Are Resistant to Diet-Induced Obesity and Insulin Resistance but Have Low Bone Density. PLoS One 7, 1–12.

Ables GP, Ouattara A, Hampton TG, Cooke D, Perodin F, Augie I, and Orentreich DS (2015). Dietary methionine restriction in mice elicits an adaptive cardiovascular response to hyperhomocysteinemia. Sci. Rep 5, 1–10.

al-Shawi R, Wallace H, Harrison S, Jones C, Johnson D, and Bishop JO (1992). Sexual dimorphism and growth hormone regulation of a hybrid gene in transgenic mice. Mol. Endocrinol 6, 181–190. [PubMed: 1373818]

Alonso C, Fernández-Ramos D, Varela-Rey M, Martínez-Arranz I, Navasa N, Van Liempd SM, Lavín Trueba JL, Mayo R, Ilisso CP, de Juan VG, et al. (2017). Metabolomic Identification of Subtypes of Nonalcoholic Steatohepatitis. Gastroenterology 152, 1449–1461.e7. [PubMed: 28132890]

Amador-Noguez D, Yagi K, Venable S, and Darlington G (2004). Gene expression profile of long-lived Ames dwarf mice and Little mice. Aging Cell 3, 423–441. [PubMed: 15569359]

Amador-Noguez D, Zimmerman J, Venable S, and Darlington G (2005). Gender-specific alterations in gene expression and loss of liver sexual dimorphism in the long-lived Ames dwarf mice. Biochem. Biophys. Res. Commun 332, 1086–1100. [PubMed: 15925325]

Anders S, and Huber W (2010). Differential expression analysis for sequence count data. Genome Biol. 11.

Baird L, and Dinkova-Kostova AT (2011). The cytoprotective role of the Keap1-Nrf2 pathway. Arch. Toxicol 85, 241–272. [PubMed: 21365312]

Balaban RS, Nemoto S, and Finkel T (2005). Mitochondria, oxidants, and aging. Cell 120, 483–495. [PubMed: 15734681]

Barger JL, Kayo T, Vann JM, Arias EB, Wang J, Hacker TA, Wang Y, Raederstorff D, Morrow JD, Leeuwenburgh C, et al. (2008). A low dose of dietary resveratrol partially mimics caloric restriction and retards aging parameters in mice. PLoS One 3.

Barger JL, Vann JM, Cray NL, Pugh TD, Mastaloudis A, Hester SN, Wood SM, Newton MA, Weindruch R, and Prolla TA (2017). Identification of tissue-specific transcriptional markers of caloric restriction in the mouse and their use to evaluate caloric restriction mimetics. Aging Cell 16, 750–760. [PubMed: 28556428]

Baur JA, and Sinclair DA (2006). Therapeutic potential of resveratrol: The in vivo evidence. Nat. Rev. Drug Discov 5, 493–506. [PubMed: 16732220]

Baur JA, Pearson KJ, Price NL, Jamieson HA, Lerin C, Kalra A, Prabhu VV, Allard JS, Lopez-Lluch G, Lewis K, et al. (2006). Resveratrol improves health and survival of mice on a high-calorie diet. Nature 444, 337–342. [PubMed: 17086191]

Baze MM, Schlauch K, and Hayes JP (2010a). Gene expression of the liver in response to chronic hypoxia. 275–288.

Baze MM, Schlauch K, and Hayes JP (2010b). Gene expression of the liver in response to chronic hypoxia. Physiol Genomics 41, 275–288. [PubMed: 20103700]

Benjamini Y, and Hochberg Y (1995). Controlling the False Discovery Rate: A Practical and Powerful Approach to Multiple Testing. J. R. Stat. Soc. Ser. B 57, 289–300.

Bolger AM, Lohse M, and Usadel B (2014). Trimmomatic: A flexible trimmer for Illumina sequence data. Bioinformatics 30, 2114–2120. [PubMed: 24695404]

Boylston WH, DeFord JH, and Papaconstantinou J (2006). Identification of longevity-associated genes in long-lived Snell and Ames dwarf mice. Age (Omaha). 28, 125–144.

Brown-borg HM (2007). Hormonal regulation of longevity in mammals. Ageing Res. Rev 6, 28–45. [PubMed: 17360245]

Brown-Borg HM, Rakoczy SG, and Uthus EO (2005). Growth hormone alters methionine and glutathione metabolism in Ames dwarf mice. Mech. Ageing Dev 126, 389–398. [PubMed: 15664625]

Buckley DB, and Klaassen CD (2009). Mechanism of Gender-Divergent UDP-Glucuronosyltransferase mRNA Expression in Mouse Liver and Kidney. 37, 834–840.

Cao L, Li W, Kim S, Brodie SG, and Deng CX (2003). Senescence, aging, and malignant transformation mediated by p53 in mice lacking the brca1 full-length isoform. Genes Dev. 17, 201–213. [PubMed: 12533509]

Chang W, Cheng J, Allaire J, Xie Y, and McPherson J (2016). shiny: Web Application Framework for R. R Packag. Version 0.14.2. Https//CRAN.R-Project.Org/Package=shiny.

Chen D, Thomas EL, and Kapahi P (2009). HIF-1 modulates dietary restriction-mediated lifespan extension via IRE-1 in *Caenorhabditis elegans*. PLoS Genet. 5.

Chresta CM, Davies BR, Hickson I, Harding T, Cosulich S, Critchlow SE, Vincent JP, Ellston R, Jones D, Sini P, et al. (2010). AZD8055 is a potent, selective, and orally bioavailable ATP-competitive mammalian target of rapamycin kinase inhibitor with in vitro and in vivo antitumor activity. Cancer Res. 70, 288–298. [PubMed: 20028854]

Collino S, Martin F-PJ, Montoliu I, Barger JL, Da Silva L, Prolla TA, Weindruch R, and Kochhar S (2013). Transcriptomics and Metabonomics Identify Essential Metabolic Signatures in Calorie Restriction (CR) Regulation across Multiple Mouse Strains. Metabolites 3, 881–911. [PubMed: 24958256]

Cort WM (1974). Antioxidant activity of tocopherols, ascorbyl palmitate, and ascorbic acid and their mode of action. J. Am. Oil Chem. Soc 51, 321–325. [PubMed: 4845640]

Coschigano KT, Clemmons D, Bellush LL, and Kopchick JJ (2000). Assessment of growth parameters and lifespan of GHR/BP gene-disrupted mice. Endocrinology 141, 2608–2613. [PubMed: 10875265]

Coschigano KT, Holland AN, Riders ME, List EO, Flyvbjerg A, and Kopchick JJ (2003). Deletion, but not antagonism, of the mouse growth hormone receptor results in severely decreased body weights, insulin, and insulin-like growth factor I levels and increased life span. Endocrinology 144, 3799–3810. [PubMed: 12933651]

David J, Van Herrewege J, and Fouillet P (1971). Quantitative under-feeding of drosophila: Effects on adult longevity and fecundity. Exp. Gerontol 6, 249–257. [PubMed: 5165170]

Dhahbi JM, Mote PL, Fahy GM, and Spindler SR (2005). Identification of potential caloric restriction mimetics by microarray profiling. Am. Physiol. Soc 23, 343–350.

Dobin A, Davis CA, Schlesinger F, Drenkow J, Zaleski C, Jha S, Batut P, Chaisson M, and Gingeras TR (2013). STAR: Ultrafast universal RNA-seq aligner. Bioinformatics 29, 15–21. [PubMed: 23104886]

Edgar R (2002). Gene Expression Omnibus: NCBI gene expression and hybridization array data repository. Nucleic Acids Res. 30, 207–210. [PubMed: 11752295]

Edwards MG, Anderson RM, Yuan M, Kendziorski CM, Weindruch R, and Prolla TA (2007). Gene expression profiling of aging reveals activation of a p53-mediated transcriptional program. BMC Genomics 8, 80. [PubMed: 17381838]

Estep PW, Warner JB, and Bulyk ML (2009). Short-term calorie restriction in male mice feminizes gene expression and alters key regulators of conserved aging regulatory pathways. PLoS One 4.

Flurkey K, Papaconstantinou J, Miller RA, and Harrison DE (2001). Lifespan extension and delayed immune and collagen aging in mutant mice with defects in growth hormone production. Proc. Natl. Acad. Sci 98, 6736–6741. [PubMed: 11371619]

Fok WC, Chen Y, Bokov A, Zhang Y, Salmon AB, Diaz V, Javors M, Wood WH, Zhang Y, Becker KG, et al. (2014a). Mice fed rapamycin have an increase in lifespan associated with major changes in the liver transcriptome. PLoS One 9.

Fok WC, Bokov A, Gelfond J, Yu Z, Zhang Y, Doderer M, Chen Y, Javors M, Wood WH, Zhang Y, et al. (2014b). Combined treatment of rapamycin and dietary restriction has a larger effect on the transcriptome and metabolome of liver. Aging Cell 13, 311–319. [PubMed: 24304444]

Fontana L, Partridge L, and Longo VD (2010). Extending Healthy Life Span—From Yeast to Humans. Science (80-.). 328, 321–326.

Fu ZD, and Klaassen CD (2014). Short-term calorie restriction feminizes the mRNA profiles of drug metabolizing enzymes and transporters in livers of mice. Toxicol. Appl. Pharmacol 274, 137–146. [PubMed: 24240088]

Fushan AA, Turanov AA, Lee SG, Kim EB, Lobanov AV, Yim SH, Buffenstein R, Lee SR, Chang KT, Rhee H, et al. (2015). Gene expression defines natural changes in mammalian lifespan. Aging Cell 14, 352–365. [PubMed: 25677554]

Gadó K, Domján G, Hegyesi H, and Falus A (2000). Role of interleukin-6 in the pathogenesis of multiple myeloma. Cell Biol. Int 24, 195–209. [PubMed: 10816321]

García-Martínez JM, Alessi DR, Moran J, Cosulich SC, Clarke RG, Gray A, and Chresta CM (2009). Ku-0063794 is a specific inhibitor of the mammalian target of rapamycin (mTOR). Biochem. J 421, 29–42. [PubMed: 19402821]

García-Martínez JM, Wullschleger S, Preston G, Guichard S, Fleming S, Alessi DR, and Duce SL (2011). Effect of PI3K- and mTOR-specific inhibitors on spontaneous B-cell follicular lymphomas in PTEN/LKB1-deficient mice. Br. J. Cancer 104, 1116–1125. [PubMed: 21407213]

Garratt M, Stockley P, Armstrong SD, Beynon RJ, and Hurst JL (2011). The scent of senescence: Sexual signalling and female preference in house mice. J. Evol. Biol 24, 2398–2409. [PubMed: 21848973]

Gautier H (1996). Interactions and control among metabolic of breathing rate, hypoxia, and control of breathing. 521–527.

Gertz M, Nguyen GTT, Fischer F, Suenkel B, Schlicker C, Fränzel B, Tomaschewski J, Aladini F, Becker C, Wolters D, et al. (2012). A Molecular Mechanism for Direct Sirtuin Activation by Resveratrol. PLoS One 7, 1–12.

Gokarn R, Solon-Biet SM, Cogger VC, Cooney GJ, Wahl D, McMahon AC, Mitchell JR, Mitchell SJ, Hine C, De Cabo R, et al. (2018). Long-term Dietary Macronutrients and Hepatic Gene Expression in Aging Mice. J Gerontol A Biol Sci Med Sci 00, 1–8.

Gorrini C, Baniasadi PS, Harris IS, Silvester J, Inoue S, Snow B, Joshi PA, Wakeham A, Molyneux SD, Martin B, et al. (2013). BRCA1 interacts with Nrf2 to regulate antioxidant signaling and cell survival. J. Exp. Med 210, 1529–1544. [PubMed: 23857982]

Grandison RC, Piper MDW, and Partridge L (2009). Amino acid imbalance explains extension of lifespan by dietary restriction in Drosophila. Nature 462, 1061–1064. [PubMed: 19956092]

De Haes W, Frooninckx L, Van Assche R, Smolders A, Depuydt G, Billen J, Braeckman BP, Schoofs L, and Temmerman L (2014). Metformin promotes lifespan through mitohormesis via the peroxiredoxin PRDX-2. Proc. Natl. Acad. Sci 111, E2501–E2509. [PubMed: 24889636]

Harrison DE, Strong R, Sharp ZD, Nelson JF, Astle CM, Flurkey K, Nadon NL, Wilkinson JE, Frenkel K, Carter CS, et al. (2009). Rapamycin fed late in life extends lifespan in genetically heterogeneous mice. Nature 460, 392–395. [PubMed: 19587680]

Harrison DE, Strong R, Allison DB, Ames BN, Astle CM, Atamna H, Fernandez E, Flurkey K, Javors MA, Nadon NL, et al. (2014). Acarbose, 17-α-estradiol, and nordihydroguaiaretic acid extend mouse lifespan preferentially in males. Aging Cell 13, 273–282. [PubMed: 24245565]

Hashimshony T, Senderovich N, Avital G, Klochendler A, de Leeuw Y, Anavy L, Gennert D, Li S, Livak KJ, Rozenblatt-Rosen O, et al. (2016). CEL-Seq2: Sensitive highly-multiplexed single-cell RNA-Seq. Genome Biol. 17, 1–7. [PubMed: 26753840]

Hine C, Harputlugil E, Zhang Y, Ruckenstuhl C, Lee BC, Brace L, Longchamp A, Treviño-Villarreal JH, Mejia P, Ozaki CK, et al. (2015). Endogenous hydrogen sulfide production is essential for dietary restriction benefits. Cell 160, 132–144. [PubMed: 25542313]

Hofmann JW, Zhao X, De Cecco M, Peterson AL, Pagliaroli L, Manivannan J, Hubbard GB, Ikeno Y, Zhang Y, Feng B, et al. (2015). Reduced expression of MYC increases longevity and enhances healthspan. Cell 160, 477–488. [PubMed: 25619689]

Houthoofd K, and Vanfleteren JR (2006). The longevity effect of dietary restriction in *Caenorhabditis elegans*. Exp. Gerontol 41, 1026–1031. [PubMed: 16782293]

Huang DW, Sherman BT, and Lempicki RA (2009a). Bioinformatics enrichment tools: Paths toward the comprehensive functional analysis of large gene lists. Nucleic Acids Res. 37, 1–13. [PubMed: 19033363]

Huang DW, Lempicki R. a, and Sherman BT (2009b). Systematic and integrative analysis of large gene lists using DAVID bioinformatics resources. Nat. Protoc 4, 44–57. [PubMed: 19131956]

Imaoka S, Fujita S, and Funae Y (1991). Age-dependent exression of cytochrome P-450s in rat liver. BBA - Mol. Basis Dis 1097, 187–192.

Jackson KL, Palma-Rigo K, Nguyen-Huu TP, Davern PJ, and Head GA (2014). Actions of rilmenidine on neurogenic hypertension in BPH/2J genetically hypertensive mice. J. Hypertens 32, 575–586. [PubMed: 24275840]

Jain IH, Zazzeron L, Goli R, Alexa K, Schatzman-Bone S, Dhillon H, Goldberger O, Peng J, Shalem O, Sanjana NE, et al. (2016). Hypoxia as a therapy for mitochondrial disease. Science (80-.). 352, 54–61.

Kabil O, Vitvitsky V, Xie P, and Banerjee R (2011). The quantitative significance of the transsulfuration enzymes for H2S production in murine tissues. Antioxid. Redox Signal 15, 363–372. [PubMed: 21254839]

Kamataki T, Maeda K, Shimada M, Kitani K, Nagai T, and Kato R (1985). Age-Related Alteration in the Activities of Drug-Metabolizing Enzymes and Contents of Sex-Specific Forms of Cytochrome P-450 in Liver Microsomes from Male and Female Rats1. J. Pharmacol. Exp. Ther 233, 222–228. [PubMed: 3981456]

Kanfi Y, Naiman S, Amir G, Peshti V, Zinman G, Nahum L, Bar-Joseph Z, and Cohen HY (2012). The sirtuin SIRT6 regulates lifespan in male mice. Nature 483, 218–221. [PubMed: 22367546]

Kapahi P, Zid BM, and Harper T (2004). Regulation of Lifespan in Drosophila by Modulation of Genes in the TOR Signaling Pathway. Curr. Biol 14, 885–890. [PubMed: 15186745]

Kautz L, Meynard D, Monnier A, Darnaud V, Bouvet R, Wang RH, Deng C, Vaulont S, Mosser J, Coppin H, et al. (2008). Iron regulates phosphorylation of Smad1/5/8 and gene expression of Bmp6, Smad7, Id1, and Atoh8 in the mouse liver. Blood 112, 1503–1509. [PubMed: 18539898]

Knopf JL, Gallagher JF, and Held WA (1983). Differential, multihormonal regulation of the mouse major urinary protein gene family in the liver. Mol. Cell. Biol 3, 2232–2240. [PubMed: 6656765]

Kobayashi T, Shimabukuro-Demoto S, Yoshida-Sugitani R, Furuyama-Tanaka K, Karyu H, Sugiura Y, Shimizu Y, Hosaka T, Goto M, Kato N, et al. (2014). The histidine transporter SLC15A4 coordinates mTOR-dependent inflammatory responses and pathogenic antibody production. Immunity 41, 375–388. [PubMed: 25238095]

Kolesnikov N, Hastings E, Keays M, Melnichuk O, Tang YA, Williams E, Dylag M, Kurbatova N, Brandizi M, Burdett T, et al. (2015). ArrayExpress update-simplifying data submissions. Nucleic Acids Res. 43, D1113–D1116. [PubMed: 25361974]

Kristiansen OP, and Mandrup-Poulsen T (2005). Interleukin-6 and Diabetes. Diabetes 54, S114 LP–S124. [PubMed: 16306329]

Lakowski B, and Hekimi S (1998). The genetics of caloric restriction in *Caenorhabditis elegans*. Proc. Natl. Acad. Sci 95, 13091–13096. [PubMed: 9789046]

Lamb J, Crawford ED, Peck D, Modell JW, Blat IC, Wrobel MJ, Lerner J, Brunet J, Subramanian A, Ross KN, et al. (2006). The Connectivity Map : Using Gene-Expression Signatures to Connect Small Molecules, Genes, and Disease. Science (80-.). 313, 1929–1935.

Leiser SF, and Miller RA (2010). Nrf2 Signaling, a Mechanism for Cellular Stress Resistance in Long-Lived Mice. Mol. Cell. Biol 30, 871–884. [PubMed: 19933842]

Li X, Bartke A, Berryman DE, Funk K, Kopchick JJ, List EO, Sun L, and Miller RA (2013). Direct and indirect effects of growth hormone receptor ablation on liver expression of xenobiotic metabolizing genes. AJP Endocrinol. Metab 305, E942–E950.

Liao Y, Smyth GK, and Shi W (2014). FeatureCounts: An efficient general purpose program for assigning sequence reads to genomic features. Bioinformatics 30, 923–930. [PubMed: 24227677]

Lin AS, Defossez P, Guarente L, Lin S, Defossez P, and Guarentet L (2000). Requirement of NAD and SIR2 for Life-Span Extension by Calorie Restriction in *Saccharomyces cerevisiae*. Science (80-.). 289, 2126–2128.

Lopez-Otin C, Blasco MA, Partridge L, Serrano M, and Kroemer G (2013). The hallmarks of aging. Cell 153.

Ma S, Yim SH, Lee S-G, Kim EB, Lee S-R, Chang K-T, Buffenstein R, Lewis KN, Park TJ, Miller RA, et al. (2015). Organization of the Mammalian Metabolome according to Organ Function, Lineage Specialization, and Longevity. Cell Metab. 22, 332–343. [PubMed: 26244935]

Ma S, Upneja A, Galecki A, Tsai YM, Burant CF, Raskind S, Zhang Q, Zhang ZD, Seluanov A, Gorbunova V, et al. (2016). Cell culture-based profiling across mammals reveals DNA repair and metabolism as determinants of species longevity. Elife 5, 1–25.

De Magalhães JP, and Toussaint O (2004). GenAge: A genomic and proteomic network map of human ageing. FEBS Lett. 571, 243–247. [PubMed: 15280050]

Martin-Montalvo A, Mercken EM, Mitchell SJ, Palacios HH, Mote PL, Scheibye-Knudsen M, Gomes AP, Ward TM, Minor RK, Blouin M-J, et al. (2013). Metformin improves healthspan and lifespan in mice. Nat Commun. 4, 2192. [PubMed: 23900241]

Matys V (2006). TRANSFAC(R) and its module TRANSCompel(R): transcriptional gene regulation in eukaryotes. Nucleic Acids Res. 34, D108–D110. [PubMed: 16381825]

Mehta R, Steinkraus KA, Sutphin GL, Ramos FJ, S L, Huh A, Davis C, Chandler-brown D, and Kaeberlein M (2009). Proteasomal Regulation of the Hypoxic Response Modulates Aging in *C.elegans*. Science (80-.). 324, 1196–1198.

Mercken EM, Hu J, Krzysik-Walker S, Wei M, Li Y, Mcburney MW, de Cabo R, and Longo VD (2014a). SIRT1 but not its increased expression is essential for lifespan extension in caloric-restricted mice. Aging Cell 13, 193–196. [PubMed: 23941528]

Mercken EM, Mitchell SJ, Martin- A, Minor RK, Almeida M, Gomes AP, Scheibye-knudsen M, Hector H, Licata JJ, Zhang Y, et al. (2014b). SRT2104 extends survival of male mice on a standard diet and preserves bone and muscle mass. 787–796.

Miller DL, and Roth MB (2007). Hydrogen sulfide increases thermotolerance and lifespan in Caenorhabditis elegans. Proc. Natl. Acad. Sci 104, 20618–20622. [PubMed: 18077331]

Miller RA, Harrison DE, Astle CM, Floyd RA, Flurkey K, Hensley KL, Javors MA, Leeuwenburgh C, Nelson JF, Ongini E, et al. (2007). An aging Interventions Testing Program: Study design and interim report. Aging Cell 6, 565–575. [PubMed: 17578509]

Miller RA, Harrison DE, Astle CM, Baur JA, Boyd AR, De Cabo R, Fernandez E, Flurkey K, Javors MA, Nelson JF, et al. (2011). Rapamycin, but not resveratrol or simvastatin, extends life span of genetically heterogeneous mice. Journals Gerontol. - Ser. A Biol. Sci. Med. Sci 66 A, 191–201.

Miller RA, Harrison DE, Astle CM, Fernandez E, Flurkey K, Han M, Javors MA, Li X, Nadon NL, Nelson JF, et al. (2014). Rapamycin-mediated lifespan increase in mice is dose and sex dependent and metabolically distinct from dietary restriction. Aging Cell 13, 468–477. [PubMed: 24341993]

Mitchell SJ, Madrigal-Matute J, Scheibye-Knudsen M, Fang E, Aon M, Gonzalez-Reyes JA, Cortassa S, Kaushik S, Gonzalez-Freire M, Patel B, et al. (2016). Effects of Sex, Strain, and Energy Intake on Hallmarks of Aging in Mice. Cell Metab. 23, 1093–1112. [PubMed: 27304509]

Moorad JA, Promislow DEL, Nate F, and Miller Richard A (2012). A comparative assessment of univariate longevity measures using zoological animal records. Aging Cell 11, 940–948. [PubMed: 22805302]

Mpoy M, Vandeleene B, Ketelslegers JM, and Lambert AE (1988). Treatment of systemic hypertension in insulin-treated diabetes mellitus with rilmenidine. Am. J. Cardiol 61, 5–8.

Mutter FE, Park BK, and Copple IM (2015). Value of monitoring Nrf2 activity for the detection of chemical and oxidative stress. Biochem. Soc. Trans 43, 657–662. [PubMed: 26551708]

Nakamura N, Lill JR, Phung Q, Jiang Z, Bakalarski C, De Mazière A, Klumperman J, Schlatter M, Delamarre L, and Mellman I (2014). Endosomes are specialized platforms for bacterial sensing and NOD2 signalling. Nature 509, 240–244. [PubMed: 24695226]

Narod SA, and Foulkes WD (2004). BRCA1 and BRCA2: 1994 and beyond. Nat. Rev. Cancer 4, 665–676. [PubMed: 15343273]

Osburn WO, Yates MS, Dolan PD, Chen S, Liby KT, Sporn MB, Taguchi K, Yamamoto M, and Kensler TW (2008). Genetic or pharmacologic amplification of Nrf2 signaling inhibits acute inflammatory liver injury in mice. Toxicol. Sci 104, 218–227. [PubMed: 18417483]

Paynter NP, Balasubramanian R, Giulianini F, Wang DD, Tinker LF, Gopal S, Deik AA, Albert CM, Clish CB, and Rexrode KM (2018). Metabolic Predictors of Incident Coronary Heart Disease in Women. Circulation 137, 841–853. [PubMed: 29459470]

Pearson KJ, Baur JA, Lewis KN, Peshkin L, Price NL, Labinskyy N, Swindell WR, Kamara D, Minor RK, Perez E, et al. (2008). Resveratrol Delays Age-Related Deterioration and Mimics Transcriptional Aspects of Dietary Restriction without Extending Life Span. Cell Metab. 8, 157–168. [PubMed: 18599363]

Plank M, Wuttke D, van Dam S, Clarke SA, and de Magalhães JP (2012). A meta-analysis of caloric restriction gene expression profiles to infer common signatures and regulatory mechanisms. Mol. Biosyst 8, 1339. [PubMed: 22327899]

Ramadoss P, Chiappini F, Bilban M, and Hollenberg AN (2010). Regulation of hepatic six transmembrane epithelial antigen of prostate 4 (STEAP4) expression by STAT3 and CCAAT/enhancer-binding protein α. J. Biol. Chem 285, 16453–16466. [PubMed: 20304921]

Rhoads TW, Burhans MS, Chen VB, Coon JJ, Colman RJ, Anderson RM, Rhoads TW, Burhans MS, Chen VB, Hutchins PD, et al. (2018). Caloric Restriction Engages Hepatic RNA Processing Mechanisms in Rhesus Monkeys Resource Caloric Restriction Engages Hepatic RNA Processing Mechanisms in Rhesus Monkeys. Cell Metab. 27, 677–688.e5. [PubMed: 29514073]

Richie JP, Leutzinger Y, Parthasarathy S, Malloy V, Orentreich N, and Zimmerman J. a (1994). Methionine restriction increases blood glutathione and longevity in F344 rats. FASEB J. 8, 1302–1307. [PubMed: 8001743]

Ritchie ME, Phipson B, Wu D, Hu Y, Law CW, Shi W, and Smyth GK (2015). Limma powers differential expression analyses for RNA-sequencing and microarray studies. Nucleic Acids Res. 43, e47. [PubMed: 25605792]

Roberts SA, Simpson DM, Armstrong SD, Davidson AJ, Robertson DH, McLean L, Beynon RJ, and Hurst JL (2010). Darcin: A male pheromone that stimulates female memory and sexual attraction to an individual male's odour. BMC Biol. 8.

Robinson MD, McCarthy DJ, and Smyth GK (2009). edgeR: A Bioconductor package for differential expression analysis of digital gene expression data. Bioinformatics 26, 139–140. [PubMed: 19910308]

Rowland JE, Lichanska AM, Linda M, White M, Aniello EM, Maher SL, Brown R, Teasdale RD, Noakes PG, Waters MJ, et al. (2005). In Vivo Analysis of Growth Hormone Receptor Signaling Domains and Their Associated Transcripts In Vivo Analysis of Growth Hormone Receptor Signaling Domains and Their Associated Transcripts. Mol. Cell. Biol 25, 66–77. [PubMed: 15601831]

Rusli F, Boekschoten MV, Zubia AA, Lute C, Müller M, and Steegenga WT (2015). A weekly alternating diet between caloric restriction and medium fat protects the liver from fatty liver development in middle-aged C57BL/6J mice. Mol. Nutr. Food Res 59, 533–543. [PubMed: 25504628]

Selman C, Kerrison ND, Cooray A, Piper MDW, Lingard SJ, Barton RH, Schuster EF, Blanc E, Gems D, Nicholson JK, et al. (2006). Coordinated multitissue transcriptional and plasma metabonomic profiles following acute caloric restriction in mice. Physiol. Genomics 27, 187–200. [PubMed: 16882887]

Selman C, Tullet JMA, Wieser D, Irvine E, Lingard SJ, Choudhury AI, Claret M, Alqassab H, Carmignac D, Ramadani F, et al. (2009). Ribosomal Protein S6 Kinase 1 Signaling Regulates Mammalian Life Span. Science (80-.). 326, 140–144.

Senn JJ, Klover PJ, Nowak IA, and Mooney RA (2002). Interleukin-6 induces cellular insulin resistance in hepatocytes. Diabetes 51, 3391–3399. [PubMed: 12453891]

Shannon P, Markiel A, Ozier Owen, 2, Baliga NS, Wang JT, Ramage D, Amin N, Schwikowski B, and Ideker T (2003). Cytoscape: a software environment for integrated models of biomolecular interaction networks. Genome Res. 2498–2504. [PubMed: 14597658]

Soo S, Kyung K, Choi M, Kim S, Park T, Cheol I, Won J, Cheol L, and Lee K (2015). Whole - transcriptome analysis of mouse adipose tissue in response to short - term caloric restriction. Mol. Genet. Genomics

Steiner AA, and Branco LGS (2002). Hypoxia-Induced Anapyrexia: Implications and Putative Mediators. Annu. Rev. Physiol 64, 263–288. [PubMed: 11826270]

Streeper RS, Grueter CA, Salomonis N, Cases S, Levin MC, Koliwad SK, Zhou P, Hirschey MD, Verdin E, and Farese RV (2012). Deficiency of the lipid synthesis enzyme, DGAT1, extends longevity in mice. Aging (Albany. NY). 4, 13–27. [PubMed: 22291164]

Strong R, Miller RA, Astle CM, Floyd RA, Flurkey K, Hensley KL, Javors MA, Leeuwenburgh C, Nelson JF, Ongini E, et al. (2008). Nordihydroguaiaretic acid and aspirin increase lifespan of genetically heterogeneous male mice. Aging Cell 7, 641–650. [PubMed: 18631321]

Strong R, Miller RA, Astle CM, Baur JA, De Cabo R, Fernandez E, Guo W, Javors M, Kirkland JL, Nelson JF, et al. (2013). Evaluation of resveratrol, green tea extract, curcumin, oxaloacetic acid, and medium-chain triglyceride oil on life span of genetically heterogeneous mice. Journals Gerontol. - Ser. A Biol. Sci. Med. Sci 68, 6–16.

Strong R, Miller RA, Antebi A, Astle CM, Bogue M, Denzel MS, Fernandez E, Flurkey K, Hamilton KL, Lamming DW, et al. (2016). Longer lifespan in male mice treated with a weakly estrogenic agonist, an antioxidant, an α-glucosidase inhibitor or a Nrf2-inducer. Aging Cell 15, 872–884. [PubMed: 27312235]

Subramanian A, Tamayo P, Mootha VK, Mukherjee S, Ebert BL, Gillette M. a, Paulovich A, Pomeroy SL, Golub TR, Lander ES, et al. (2005). Gene set enrichment analysis: a knowledge-based approach for interpreting genome-wide expression profiles. Proc. Natl. Acad. Sci. U. S. A 102, 15545–15550. [PubMed: 16199517]

Subramanian A, Narayan R, Corsello SM, Peck DD, Natoli TE, Lu XL, Gould J, Doench JG, Bittker JA, Root DE, et al. (2017). A Next Generation Connectivity Map: L1000 platform and the first 1,000,000 profiles. Cell 171, 1437–1452. [PubMed: 29195078]

Sun LY, Spong A, Swindell WR, Fang Y, Hill C, Huber JA, Boehm JD, Westbrook R, Salvatori R, and Bartke A (2013). Growth hormone-releasing hormone disruption extends lifespan and regulates response to caloric restriction in mice. Elife 2, e01098. [PubMed: 24175087]

Swardfager W, Lanctt K, Rothenburg L, Wong A, Cappell J, and Herrmann N (2010). A meta-analysis of cytokines in Alzheimer's disease. Biol. Psychiatry 68, 930–941. [PubMed: 20692646]

Swindell WR (2008). Comparative analysis of microarray data identifies common responses to caloric restriction among mouse tissues. Mech. Ageing Dev 129, 138–153. [PubMed: 18155270]

Sykiotis GP, and Bohmann D (2008). Keap1/Nrf2 Signaling Regulates Oxidative Stress Tolerance and Lifespan in Drosophila. Dev. Cell 14, 76–85. [PubMed: 18194654]

Sziráki A, Tyshkovskiy A, and Gladyshev VN (2018). Global remodeling of the mouse DNA methylome during aging and in response to calorie restriction. Aging Cell e12738. [PubMed: 29575528]

Tissenbaum H. a, and Guarente L (2001). Increased dosage of a sir-2 gene extends lifespan in *Caenorhabditis elegans*. Nature 410, 227–230. [PubMed: 11242085]

Tsuchiya T, Dhahbi JM, Cui X, Mote PL, Bartke A, and Spindler SR (2004). Additive regulation of hepatic gene expression by dwarfism and caloric restriction. Physiol. Genomics 17, 307–315. [PubMed: 15039484]

Tullet JMA, Hertweck M, An JH, Baker J, Hwang JY, Liu S, Oliveira RP, Baumeister R, and Blackwell TK (2008). Direct Inhibition of the Longevity-Promoting Factor SKN-1 by Insulin-like Signaling in *C. elegans*. Cell 132, 1025–1038. [PubMed: 18358814]

Ubagai T, Lei KJ, Huang S, Mudd SH, Levy HL, and Chou JY (1995). Molecular mechanisms of an inborn error of methionine pathway. Methionine adenosyltransferase deficiency. J. Clin. Invest 96, 1943–1947. [PubMed: 7560086]

Uthus EO, and Brown-Borg HM (2003). Altered methionine metabolism in long living Ames dwarf mice. Exp. Gerontol 38, 491–498. [PubMed: 12742526]

Valenzano DR, Terzibasi E, Genade T, Cattaneo A, Domenici L, and Cellerino A (2006). Resveratrol prolongs lifespan and retards the onset of age-related markers in a short-lived vertebrate. Curr. Biol 16, 296–300. [PubMed: 16461283]

Vellai T, Takacs-Vellai K, Zhang Y, Kovacs AL, Orosz L, and Müller F (2003). Genetics: influence of TOR kinase on lifespan in *C. elegans*. Nature 426, 620.

Veurink G, Liu D, Taddei K, Perry G, Smith MA, Robertson TA, Hone E, Groth DM, Atwood CS, and Martins RN (2003). Reduction of inclusion body pathology in ApoE-deficient mice fed a combination of antioxidants. Free Radic. Biol. Med 34, 1070–1077. [PubMed: 12684092]

Viechtbauer W (2010). Conducting Meta-Analyses in R with the metafor Package. J. Stat. Softw 36, 1–48.

Viswanathan M, Kim SK, Berdichevsky A, and Guarente L (2005). A role for SIR-2.1 regulation of ER stress response genes in determining *C. elegans* life span. Dev. Cell 9, 605–615. [PubMed: 16256736]

Wauthier V, Verbeeck R, and Buc Calderon P (2007). The Effect of Ageing on Cytochrome P450 Enzymes: Consequences for Drug Biotransformation in the Elderly. Curr. Med. Chem 14, 745–757. [PubMed: 17346160]

Waxman DJ, and Holloway MG (2009). Sex Differences in the Expression of Hepatic Drug Metabolizing Enzymes. Mol Pharmacol 76, 215–228. [PubMed: 19483103]

Weindruch R, Walford RL, Fligiel S, and Guthrie D (1986). The retardation of aging in mice by dietary restriction: longevity, cancer, immunity and lifetime energy intake. J. Nutr 116, 641–654. [PubMed: 3958810]

Wood JG, Regina B, Lavu S, Hewitz K, Helfand SL, Tatar M, and Sinclair D (2004). Sirtuin activators mimic caloric restriction and delay ageing in metazoans. Nature 430, 686–689. [PubMed: 15254550]

Yongxi T, Haijun H, Jiaping Z, Guoliang S, and Hongying P (2015). Autophagy inhibition sensitizes KU-0063794-mediated anti-HepG2 hepatocellular carcinoma cell activity in vitro and in vivo. Biochem. Biophys. Res. Commun 465, 494–500. [PubMed: 26278819]

Yuan R, Tsaih S, Petkova SB, De Evsikova CM, Marion MA, Bogue MA, Mills KD, Peters LL, Bult CJ, Rosen CJ, et al. (2009). Aging in inbred strains of mice: Study design and interim report on median lifespan and circulating IGF1 levels. Aging Cell 8, 277–287. [PubMed: 19627267]

Zahn JM, Sonu R, Vogel H, Crane E, Mazan-Mamczarz K, Rabkin R, Davis RW, Becker KG, Owen AB, and Kim SK (2006). Transcriptional profiling of aging in human muscle reveals a common aging signature. PLoS Genet. 2, 1058–1069.

Zhang L, Ebenezer PJ, Dasuri K, Fernandez-Kim SO, Francis J, Mariappan N, Gao Z, Ye J, Bruce-Keller AJ, and Keller JN (2011). Aging is associated with hypoxia and oxidative stress in adipose tissue: implications for adipose function. Am. J. Physiol. Endocrinol. Metab 301, E599–607. [PubMed: 21586698]

Zhang Y, Xie Y, Berglund ED, Colbert Coate K, He TT, Katafuchi T, Xiao G, Potthoff MJ, Wei W, Wan Y, et al. (2012). The starvation hormone, fibroblast growth factor-21, extends lifespan in mice. Elife 2012, 1–14.

Zhao Y, Tyshkovskiy A, Muñoz-Espín D, Tian X, Serrano M, de Magalhaes JP, Nevo E, Gladyshev VN, Seluanov A, and Gorbunova V (2018). Naked mole rats can undergo developmental, oncogene-induced and DNA damage-induced cellular senescence. Proc. Natl. Acad. Sci 115, 1801–1806. [PubMed: 29432174]

Zhou B, Yang L, Li S, Huang J, Chen H, Hou L, Wang J, Green CD, Yan Z, Huang X, et al. (2012). Midlife gene expressions identify modulators of aging through dietary interventions. Proc. Natl. Acad. Sci. U. S. A 109, E1201–9. [PubMed: 22509016]

Zhou Y, Xu BC, Maheshwari HG, He L, Reed M, Lozykowski M, Okada S, Cataldo L, Coschigamo K, Wagner TE, et al. (1997). A mammalian model for Laron syndrome produced by targeted disruption of the mouse growth hormone receptor/binding protein gene (the Laron mouse). Proc. Natl. Acad. Sci. U. S. A 94, 13215–13220. [PubMed: 9371826]

CONTEXT AND SIGNIFICANCE

Many interventions are known that extend the lifespan of mammals, including drugs, diets and genetic manipulations. However, a systematic understanding of the general principles of lifespan control is lacking. Tyshkovskiy et al. performed a comprehensive analysis of existing lifespan-extending interventions and their effect on gene expression in mice. They discovered that certain patterns of gene expression are associated with longevity regardless of the intervention type. Researchers then used these ‘longevity signatures’ to predict candidate lifespan-extending drugs. It may be possible to one day translate these findings to maximize human lifespan and delay the effects of aging.

HIGHLIGHTS

- Sex-specific differences are decreased in response to longevity interventions
- Many interventions, but not rapamycin, exhibit similar transcriptomic responses
- Certain gene expression changes are associated with longevity across interventions
- Longevity signatures may be used to discover new lifespan-extending interventions

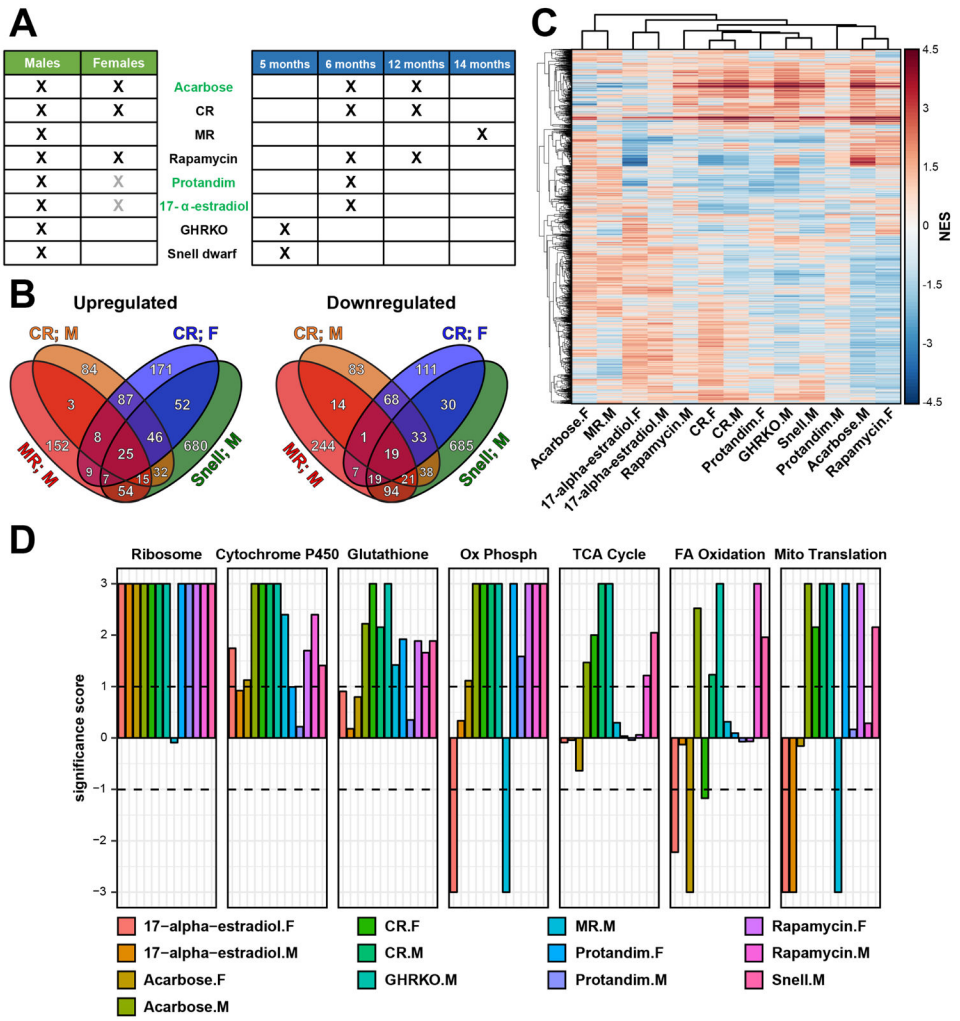

Figure 1. RNAseq of mouse hepatic response to longevity interventions

(A) RNAseq dataset. X denotes utilized experimental designs (n=3 for each group). Interventions, which have not been previously analyzed at the level of gene expression, are colored in green. Grey X marks denote experimental designs that failed to extend lifespan with statistical significance.

(B) Overlap of significant gene expression changes in response to longevity interventions.

(C) Functions enriched by genes changed in response to lifespan-extending interventions. Normalized enrichment scores (NES) of functions enriched by at least one intervention are shown.

(D) Functions enriched by up- (up) and downregulated (down) genes across interventions. Significance score, calculated as $\log_{10}$(q-value) corrected by the sign of regulation, is plotted on the y axis. FDR threshold of 0.1 is shown by dotted lines. The whole list of enriched functions is in Table S2.

Cytochrome P450: Drug metabolism by cytochrome P450; Glutathione: Glutathione metabolism; Ox Phosph: Oxidative phosphorylation; TCA cycle: Citrate Cycle/TCA Cycle; FA oxidation: Fatty acid β-oxidation; Mito Translation: Mitochondrial translation; Snell: Snell dwarf mice; F: Females; M: Males.

See also Figure S1 and Tables S1 and S2.

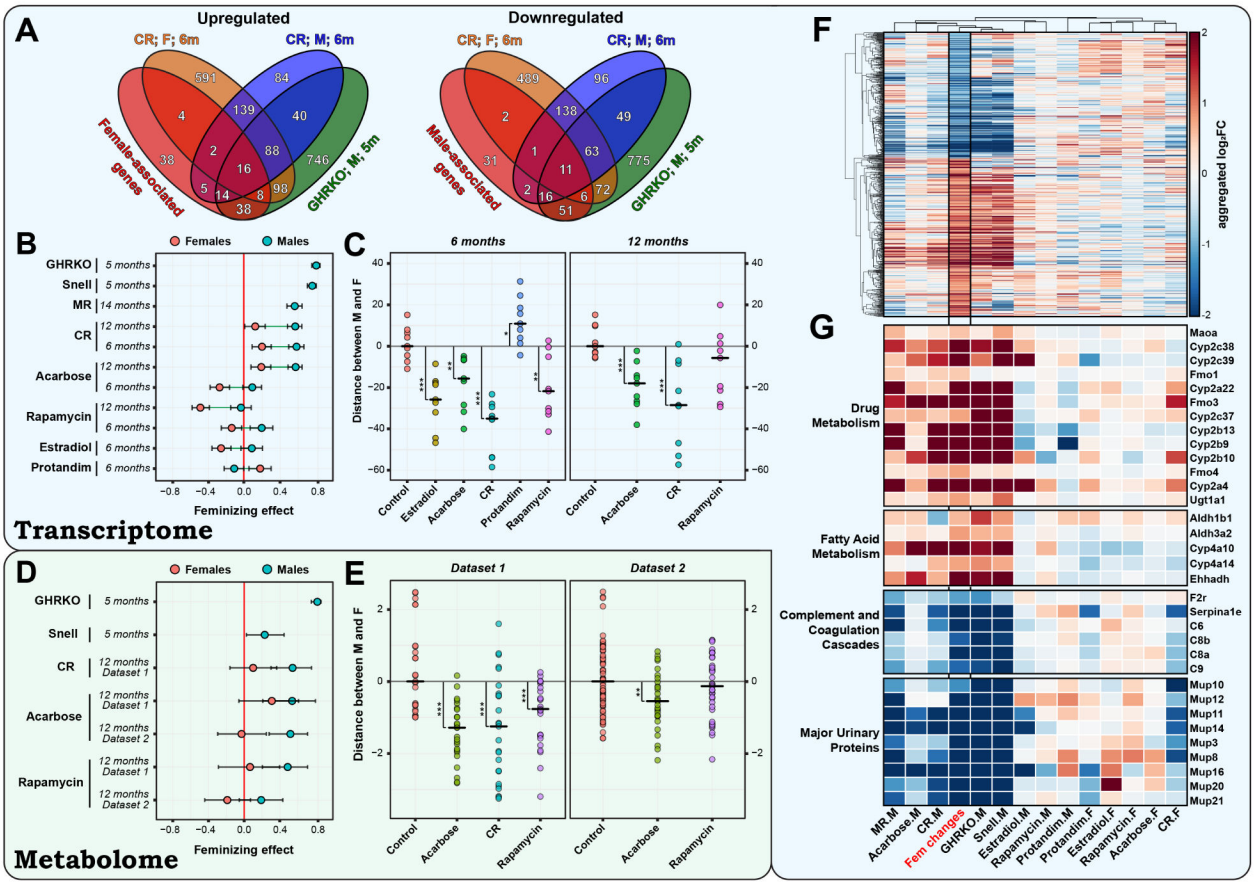

Figure 2. Feminizing effect of lifespan-extending interventions

(A) Overlap of genes differentially expressed between males and females and in response to interventions. Fisher exact test adjusted p-value < $4.1 \cdot 10^{-4}$ for overlap of all presented interventions with sex-associated genes.

(B) Feminizing effect of gene expression changes across interventions. The feminizing effect is defined as correlation between $\log_2$FC of gender-associated genes across sexes and in response to certain intervention. Error bars represent 90% confidence intervals.

(C) Diminution of gender gene expression differences by lifespan-extending interventions. Each dot represents a distance between the expression of sex-specific genes in 2 samples (corresponding to male and female). All pairwise comparisons between single samples are shown. Distances are centered around the average distance between corresponding control samples. * P.adjusted < 0.1; ** P.adjusted < 0.05; *** P.adjusted < 0.01.

(D) Feminizing effect of metabolite changes across interventions. Error bars represent 90% confidence intervals.

(E) Diminution of gender metabolome differences by lifespan-extending interventions. Each dot represents a distance between the level of sex-specific metabolites in 2 samples (corresponding to male and female). All distances are centered around the average distance between corresponding control samples. * P.adjusted < 0.1; ** P.adjusted < 0.05; *** P.adjusted < 0.01.

(F) log_2FC of genes differentially expressed between females and males (Fem changes) and in response to longevity interventions.

(G) Functional enrichment of feminizing changes across interventions. Major urinary proteins are annotated by INTERPRO, other presented functions are annotated by KEGG. Estradiol: 17-α-estradiol; Snell: Snell dwarf mice; F: Females; M: Males; 12m: 12 months; 6m: 6 months; 5m: 5 months.

See also Figure S1 and Tables S1 and S3.

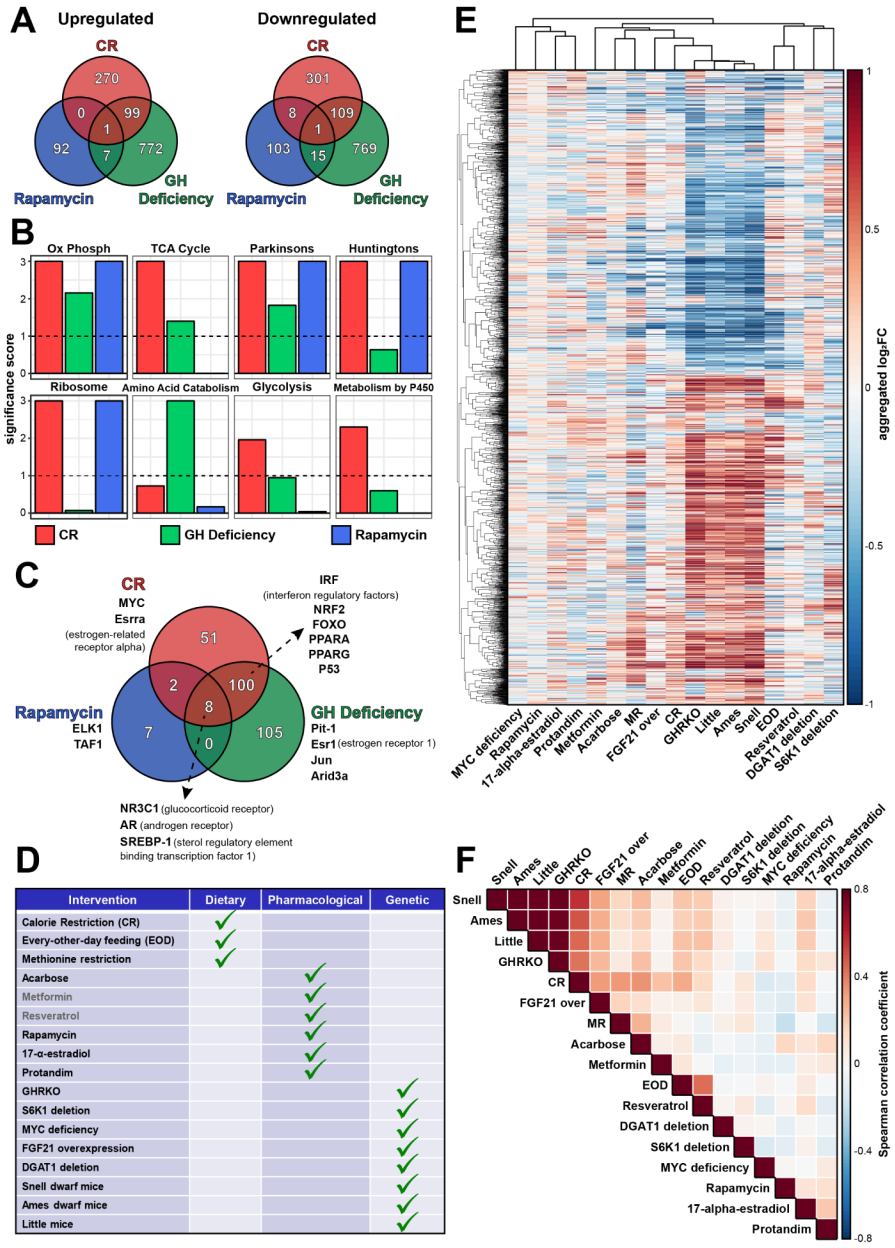

Figure 3. Gene signatures of CR, rapamycin and GH-deficiency

(A) Overlap of genes significantly up- and downregulated in response to interventions.

(B) Functional enrichment of gene signatures. Significance score, calculated as $\log_{10}$(q-value) corrected by the sign of regulation, is plotted on y axis. q-value threshold of 0.1 is shown by dotted lines. The whole list of enriched functions is in Table S4A. Ox Phosph: Oxidative phosphorylation; TCA cycle: Citrate Cycle/TCA Cycle; Parkinsons: Parkinson's Disease; Huntingtons: Huntington's Disease; Amino Acid Catabolism: Cellular Amino Acid Catabolic Process; Glycolysis: Glycolysis/Gluconeogenesis; Metabolism by P450: Drug metabolism by cytochrome P450.

(C) Overlap of transcription factors IDs enriched by gene signatures. The whole list of enriched transcription factors is in Table S5.

(D) Interventions included into meta-analysis. Two interventions shown in grey didn't significantly extend lifespan in ITP studies.

(E) Aggregated response (log_2FC) of CR, rapamycin and GH-deficiency gene signatures to different interventions. Union of genes shown in Fig. 3A were used.

(F) Spearman correlation between aggregated response of CR, rapamycin and GH-deficiency gene signatures to different interventions. Union of genes shown in Fig. 3A were used for calculation.

Snell: Snell dwarf mice; Ames: Ames dwarf mice; Little: Little mice; FGF21 over: FGF21 overexpression.

See also Figures S2 and S3 and Tables S1, S4 and S5.

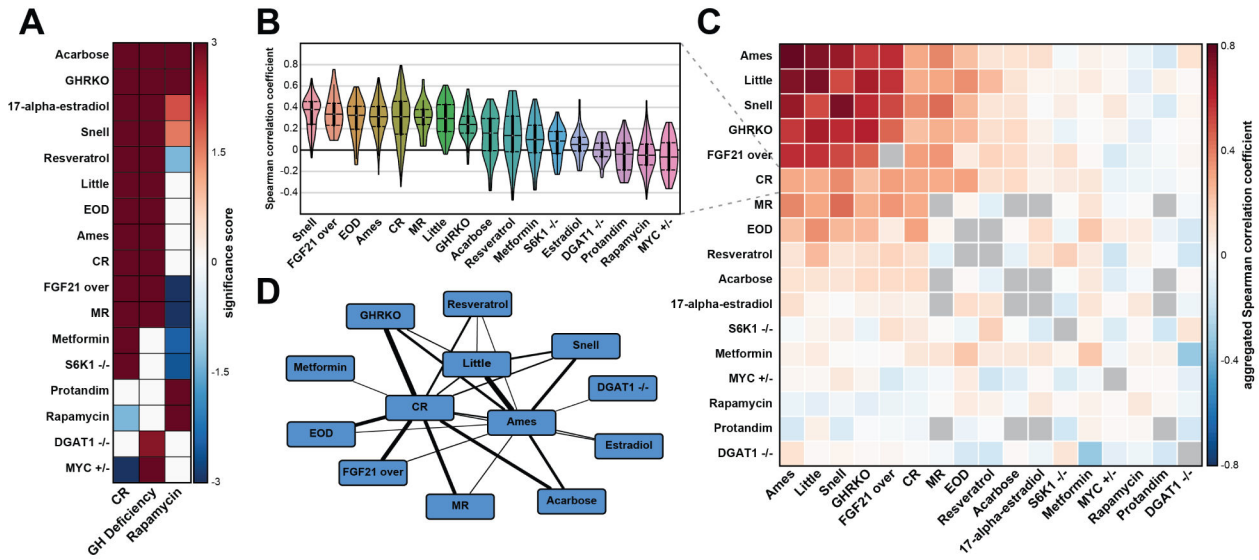

Figure 4. Mutual organization of longevity interventions

(A) Enrichment of interventions by gene signatures of CR, rapamycin and GH deficiency. Each cell represents a significance score calculated based on GSEA. Only significant associations are colored.

(B) Similarity between gene expression profiles of CR and other interventions. For every intervention, violinplot shows distribution of Spearman correlation coefficients between individual datasets.

(C) Correlation matrix of aggregated gene expression profiles across interventions. For each pair of interventions, including main diagonal, matrix represents median Spearman correlation value across all possible comparisons of individual datasets from different sources. Boxes, for which no 2 independent datasets are available, are colored in grey.

(D) Network of interventions based on similarity of their gene expression profiles. The width of edge is defined by significance of Spearman correlation between interventions. Only significant connections are shown.

Estradiol: 17-α-estradiol; Snell: Snell dwarf mice; Ames: Ames dwarf mice; FGF21 over: FGF21 overexpression; Little: Little mice.

See also Figure S4.

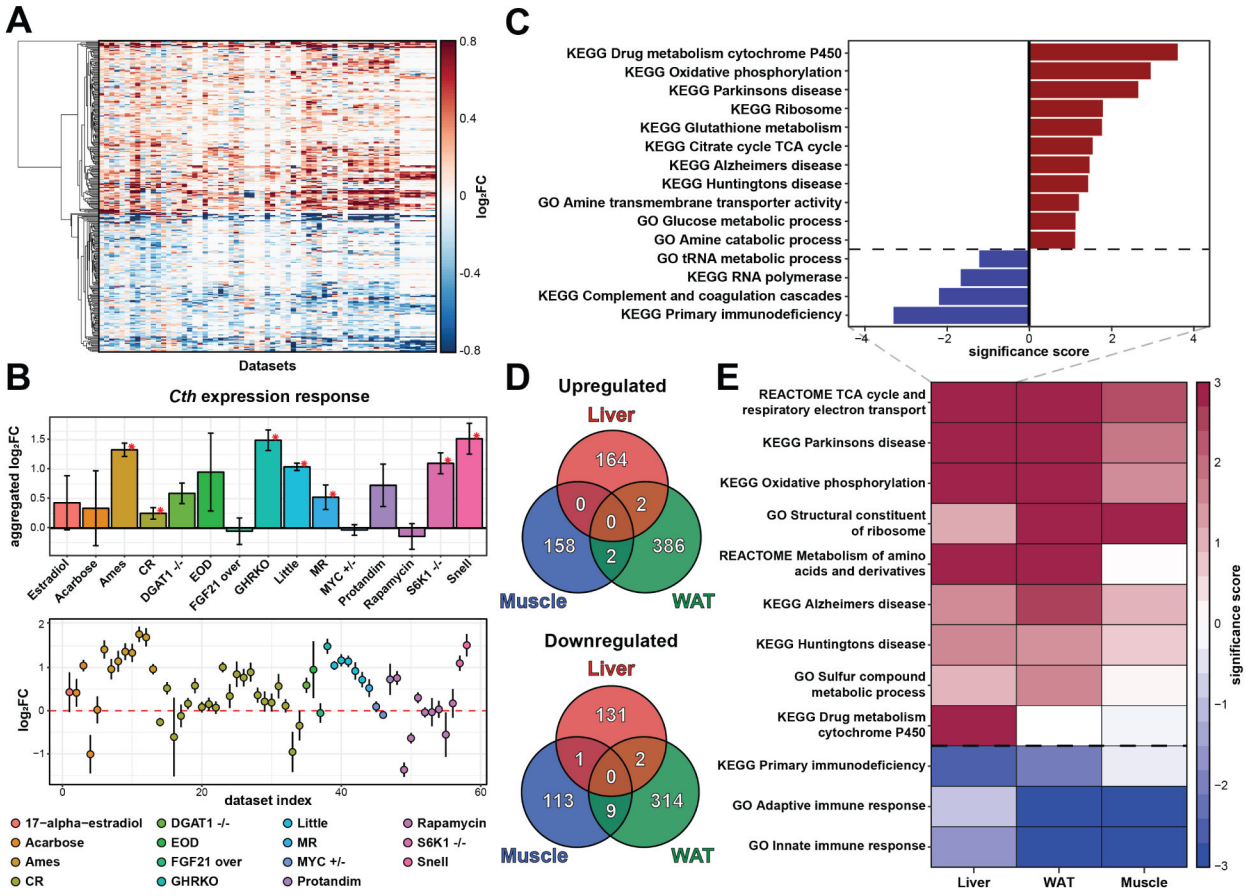

Figure 5. Common signatures of longevity interventions

(A) Fold change of genes commonly changed (166 up- and 134 downregulated) in response to interventions. X axis represents individual datasets.

(B) *Cth* expression response across interventions (upper) and individual datasets (lower). On the lower plot, dots are colored based on the type of intervention. Red asterisk: adjusted p-value < 0.05. Estradiol: 17-α-estradiol; Snell: Snell dwarf mice; Ames: Ames dwarf mice; Little: Little mice; FGF21 over: FGF21 overexpression.

(C) Functional enrichment of common longevity signatures in liver. Only enriched functions are shown. Significance score, calculated as $\log_{10}$(q-value) corrected by the sign of regulation, is presented on x-axis. The whole list of enriched functions is in Table S4B.

(D) Overlap of common longevity signatures across tissues.

(E) Functional enrichment of common longevity signatures across tissues. Only functions enriched within at least one tissue are presented. Cells are colored based on significance scores, calculated as $\log_{10}$(q-value) corrected by sign of regulation. The whole list of enriched functions is in Table S4B. Muscle: Skeletal Muscle; WAT: White Adipose Tissue.

See also Figures S5 and S6 and Tables S1, S4 and S6.

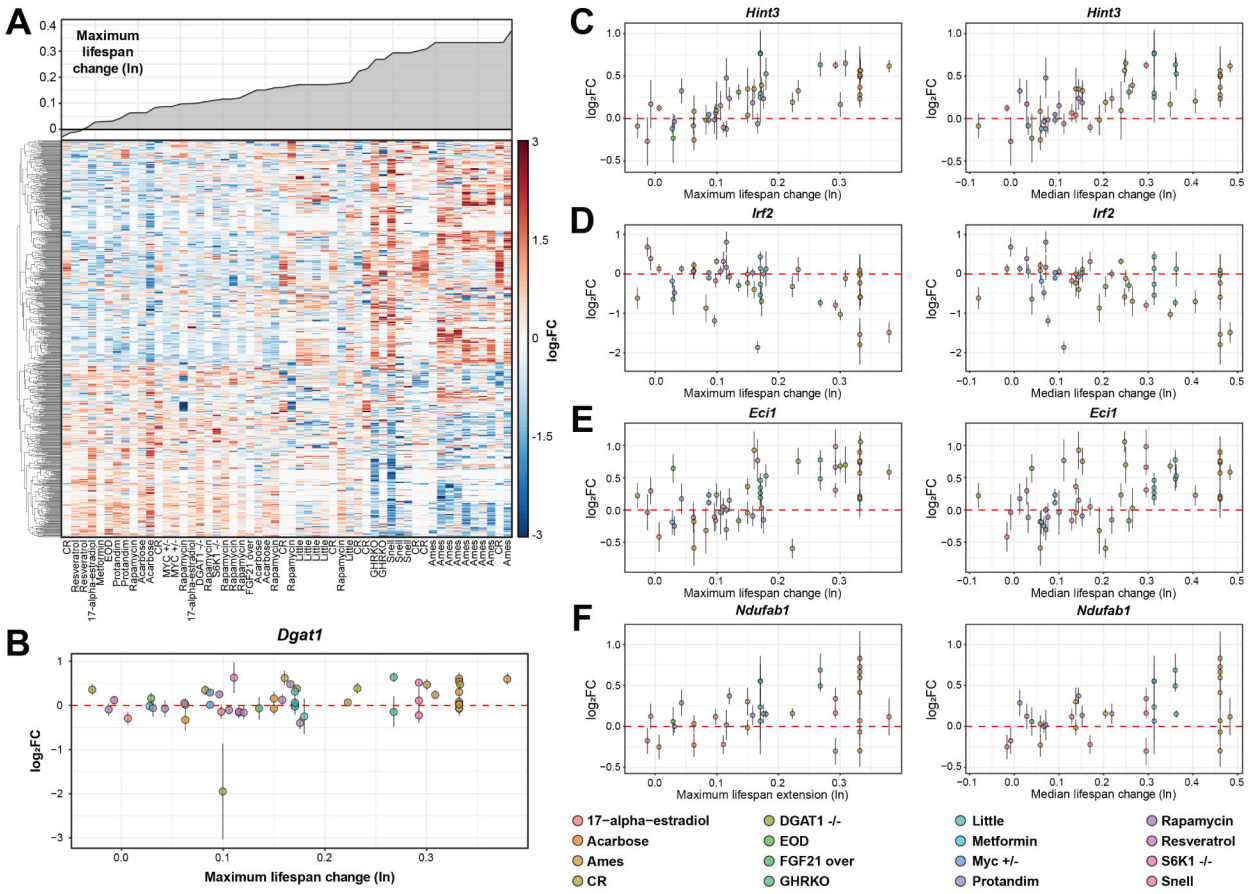

Figure 6. Gene signatures associated with the effect on lifespan

(A) Genes positively (351) and negatively (264) associated with the effect on maximum lifespan. X axis represents individual datasets. Upper plot shows the effect on maximum lifespan for the corresponding dataset.

(B) Association of *Dgat1* expression change with the effect on maximum lifespan.

(C-F) Association of *Hint1* (C), *Irf2* (D), *Eci1* (E) and *Ndufab1* (F) expression change with the effect on maximum (left) and median (right) lifespan. All specified genes are significantly associated with both metrics.

FGF21 over: FGF21 overexpression; Snell: Snell dwarf mice; Ames: Ames dwarf mice; Little: Little mice.

See also Figure S6.

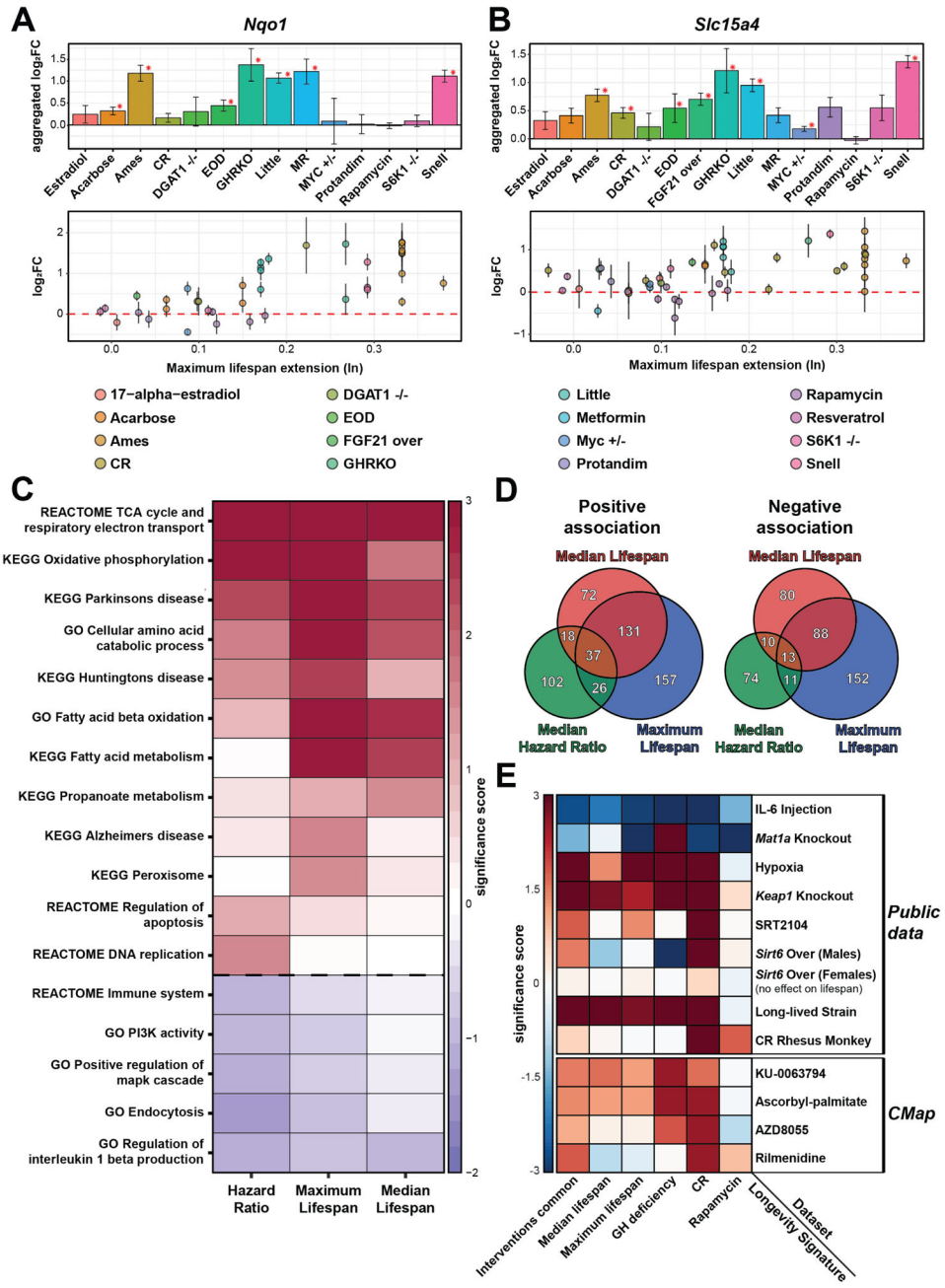

Figure 7. Persistent longevity patterns and identification of new lifespan-extending interventions

(A-B) Expression changes of *Nqo1* (A) and *Slc15a4* (B) across interventions (upper) and against the effect on maximum lifespan (lower). Red asterisk: adjusted p-value < 0.1. Estradiol: 17-α-estradiol; Snell: Snell dwarf mice; Ames: Ames dwarf mice; Little: Little mice; FGF21 over: FGF21 overexpression.

(C) Functional enrichment of genes associated with lifespan extension effect. Only functions significantly associated with at least one lifespan extension metric are shown. Cells are colored based on significance score, calculated as $\log_{10}$(q-value) corrected by the sign of regulation. The whole list of enriched functions is in Table S4C.

(D) Overlap of genes positively (left) and negatively (right) associated with effect on different metrics of lifespan. Fisher exact test p-value < 10^{-18} for all pairwise comparisons. **(E) Association of gene expression profiles of interventions from public sources (upper) and predicted by CMap (lower) with identified longevity signatures.** The latter include gene signatures of individual interventions (CR, rapamycin and GH deficiency), common signatures (Interventions common) and signatures associated with the effect on lifespan (Maximum and median lifespan). Cells are colored based on significance score, calculated as $\log_{10}$(adjusted p-value) corrected by sign of regulation. *Sirt6* Over: *Sirt6* Overexpression. See also Tables S1, S4 and S6.

KEY RESOURCES TABLE

REAGENT or RESOURCE	SOURCE	IDENTIFIER
Chemicals, Peptides, and Recombinant Proteins		
Rapamycin	LC Laboratories	Cat#R-5000
Protandim	LifeVantage Corporation	https://www.lifevantage.com/
17-alpha-estradiol	Steraloids Inc.	Cat#E0870-000
Acarbose	Spectrum Chemical Mfg. Corp.	Cat#A3965
Ascorbyl-palmitate	MedChemExpress	Cat#HY-B0987
KU-0063794	MedChemExpress	Cat#HY-50710
AZD8055	MedChemExpress	Cat#HY-10422
Rilmenidine	AK Scientific, Inc.	Cat#H733
Critical Commercial Assays		
PureLink RNA Mini Kit	Thermo Fisher Scientific	Cat#12183020
Deposited Data		
Raw and mapped RNAseq data	This paper	GEO: GSE131901
Raw and preprocessed metabolome data (batch 1)	This paper	Data S1
Additional metabolome data (batch 2)	Ma et al., 2015	N/A
App for visualization of associations between gene expression response and longevity: GENtervention	This paper	http://gladyshevlab.org/GENtervention/
Database of genes regulating lifespan: GenAge	De Magalhães and Toussaint, 2004	http://genomics.senescence.info/genes/
Public data on gene expression in response to lifespan-extending interventions	Amador-Noguez et al., 2004; Selman et al., 2009; Amador-Noguez et al., 2005; Selman et al., 2006; Tsuchiya et al., 2004; Pearson et al., 2008; Dhahbi et al., 2005; Streeper et al., 2012; Boylston et al., 2006; Zhou et al., 2012; Zhang et al., 2012; Martin-Montalvo et al., 2013; Fok et al., 2014b; Mercken et al., 2014a; Fok et al., 2014a; Collino et al., 2013; Sun et al., 2013; Hofmann et al., 2015; Rusli et al., 2015; Edwards et al., 2007; Mitchell et al., 2016; Rowland et al., 2005; Soo et al., 2015; Barger et al., 2017; Barger et al., 2008	ArrayExpress: E-MEXP-153, E-MEXP-2320, E-MEXP-347, E-MEXP-748. GEO: GSE1093, GSE11291, GSE11845, GSE2431, GSE26267, GSE3129, GSE3150, GSE36838, GSE39313, GSE40936, GSE40977, GSE46895, GSE48331, GSE48333, GSE49000, GSE50789, GSE51108, GSE55272, GSE60596, GSE61233, GSE6323, GSE70857, GSE75574, GSE81959 and GSE988
Public data on gene expression in response to interventions for association test	Ramadoss et al., 2010; Alonso et al., 2017; Baze et al., 2010b; Osburn et al., 2008; Mercken et al., 2014b; Kautz et al., 2008; Rhoads et al., 2018; Kanfi et al., 2012	GEO: GSE21060, GSE77082, GSE15891, GSE11287, GSE49000, GSE10421 and GSE104234
Experimental Models: Organisms/Strains		
Mouse: C57BL/6J	The Jackson Laboratory	JAX 000664
Mouse: UM-HET3	Laboratory of Richard Miller (Miller et al., 2007)	N/A
Mouse: GHRKO ([C57BL/6J × BALB/cByJ]/F2)	Laboratory of Richard Miller (Coschigano et al., 2003)	N/A
Mouse: Snell dwarf mice ([DW/J × C3H/HEJ]/F2)	Laboratory of Richard Miller (Flurkey et al., 2001)	N/A
Software and Algorithms		
Mapping reads: STAR 2.5.2b	Dobin et al., 2013	https://github.com/alexdobin/STAR/releases

REAGENT or RESOURCE	SOURCE	IDENTIFIER
Counting reads: featureCounts 1.5	Liao et al., 2014	http://subread.sourceforge.net/
Adaptor removing: Trimmomatic	Bolger et al., 2014	http://www.usadellab.org/cms/index.php?page=trimmomatic
Functional enrichment: GSEA	Subramanian et al., 2005	http://software.broadinstitute.org/gsea/index.jsp
App development: shiny	Chang et al., 2016	https://shiny.rstudio.com/
Programming environment: RStudio	https://www.rstudio.com/	N/A
Enrichment by transcriptional factors: TRANSFAC	Matys, 2006	http://genexplain.com/transfac/
Network visualization: Cytoscape	Shannon et al., 2003	https://cytoscape.org/
Functional annotation: DAVID	Huang et al., 2009a, 2009b	https://david.ncifcrf.gov/
Differential gene expression analysis of RNAseq: edgeR	Robinson et al., 2009	https://bioconductor.org/packages/release/bioc/html/edgeR.html
Differential gene expression analysis of microarrays: limma	Ritchie et al., 2015	https://bioconductor.org/packages/release/bioc/html/limma.html
Mixed-effect model: metafor	Viechtbauer, 2010	http://CRAN.R-project.org/package=metafor
RNAseq normalization: RLE	Anders and Huber, 2010	https://bioconductor.org/packages/release/bioc/html/edgeR.html
Prediction of compounds with similar gene expression response: CMap	Lamb et al., 2006; Subramanian et al., 2017	https://clue.io